Analysis of Genetic Variability within the Beijing Lineage of *Mycobacterium tuberculosis*

Samuel Donato

Department of Microbiology and Immunology

McGill University, Montreal, Quebec, Canada

August 2011

A thesis submitted to McGill University in partial fulfillment of the requirements of the degree of Master of Science.

ABSTRACT

Previous research has demonstrated that the DosR/DosS two-component signaling system is constitutively overexpressed in modern Beijing strains of *Mycobacterium tuberculosis* (*M. tb*). It is hypothesized that constitutive overexpression of this regulatory system is related to the unique pathogenic properties reported for this important strain lineage. Within this thesis we attempted to determine the cause of this overexpression phenotype. We first compared known DosR signaling stimuli between different strains of *M. tb*, looking specifically at NO (nitric oxide) and redox (reduction-oxidation) balance. We demonstrated that there was no difference in endogenous NO production between strains, but we showed that there was a significantly more reductive NADH/NAD pool in modern Beijing strains. To determine the specific factor responsible, we transformed four independent strains of *M. tb* with a DosR-dependent *XylE* reporter and developed a novel colony-screening assay to determine DosR activity. We then performed whole-genome transposon mutagenesis to screen for genes that are potentially able to modify DosR expression and/or activity. After screening ~80,000 transductants, we identified 49 genes that appear to influence reporter activity. Surprisingly, when analyzed by qRT-PCR, we were not able to demonstrate a modulation in *dosR* expression for any of these putative candidates, which suggested that expression of our reporter was being modified in a DosR-independent manner. Further analysis has revealed that many candidate genes directly affect the activity of the reporter protein by modulating H_2O_2 levels within the bacteria. Intriguingly, this lead us to the observation that modern Beijing strains have elevated catalase activity compared to other strains of *M. tb*. This work further characterizes the unique properties of the Beijing lineage of *M. tb* and identifies a novel phenotype that may be associated with its pathogenesis.

RÉSUMÉ

Des recherches antérieures ont démontré que le système de signalisation DosR/DosS est surexprimé dans les souches de Beijing moderne, une sous-catégorie du *Mycobacterium tuberculosis* (*M tb*). Une hypothèse explique que la surexpression du système règlementaire est la raison des propriétés plus pathogénique de la souche Beijing moderne. Dans cette thèse, nous avons fait une tentative pour trouver la cause de la surexpression. Pour débuter, les stimuli de signalisation DosR connu a été comparé entre différentes souches de *M. tb*, en regardant spécifiquement les données concernant l'oxyde nitrique (NO) et l'équilibre d'oxydo-réduction (redox). Nous avons démontré que la production NO endogène est semblable aux autres souches. Par contre, nous avons prouvé que les souches Beijing moderne expriment une plus grande proportion de NADH/NAD, ce qui lui donne une propriété plus réduisant que les autres souches. Pour trouver l'unique facteur responsable, nous avons transformé quatre souches de *M. tb* possédant un reporteur DosR-dépendant et développé une analyse innovatrice : un criblage de colonie. Ceci a pu évaluer l'activité du DosR. Ensuite, nous avons exécuté une mutagénèse utilisant un transposon pour déterminer les gênes capables de modifier l'expression et/ou l'activité du DosR. Après l'analyse d'environ 80,000 colonies, nous avons identifié 49 gênes qui semblaient avoir influencé l'activité du reporteur. À notre surprise, vérifiant l'analyse du qRT-PCR sur nos bactéries, nous étions incapable de démontrer une modulation dans l'expression du *dosR*. Ceci suggérait donc que l'expression du reporteur était en fait modifiée de manière indépendante du DosR. De plus profondes analyses ont révélé que plusieurs gênes bactériennes, dont nous avons antérieurement identifié, jouent directement un rôle sur l'activité du reporteur en contrôlant les niveaux de H_2O_2 de la bactérie. Cette découverte a mené à la conclusion que les souches Beijing moderne ont un niveau plus élevé de catalase comparé aux autres. En outre, cette thèse s'interroge plus profondément sur les propriétés uniques de la souche Beijing moderne et identifie un nouveau phénotype qui pourrait être associé au pathogène.

ACKNOWLEDGEMENTS

I would like to thank my supervisor, Dr. Michael Reed, for the opportunity to perform research in his laboratory. I would like to thank him for the idea for my project and for all the time he dedicated to discussing and helping me to critically analyze my results. I would also like to thank him for being so hands-on, and for caring about my future.

I would like to thank Dr. Pilar Domenech for keeping the lab running and supplies available. I would also like to thank Pilar for always being available to discuss results and for help troubleshooting experiments. I would like to thank Ashley Fallow and Gaëlle Kolly for preliminary cDNA and for experimental advice. I would like to thank Fonds de la Recherche en Santé du Québec (FRSQ) for their generous financial support.

I would like to thank Fiona McIntosh for supervising the BL3 lab and keeping it organized and maintained. I would like to thank Jalal Moolji for help editing this thesis. I would also like to thank Alex Dufort and Jean-Daniel Lalande for help with experiments, editing and for always being available to talk to. I would finally like to thank my parents for personal and financial support and for Molly Lanthier for being so understanding and for always being there for me.

TABLE OF CONTENTS

LIST OF TABLES

LIST OF FIGURES

AIDS − acquired immune deficiency syndrome

BCG − bacilli Calmette-Guérin

bp – base pairs

BLAST – Basic local alignment search tool

CCM – central carbon metabolism

cfu – colony forming units

DETA/NO − diethylene triamine/nitric oxide

E. coli – *Escherichia coli*

EHR – enduring hypoxic response

ETB – Ethambutol

ETC – electron transport chain

HGT – horizontal gene transfer

HIV − human immunodeficiency virus

INH – Isoniazid

KO − knock out

LSP – large sequence polymorphism

M. tb − *Mycobacterium tuberculosis*

MDR-TB − multi-drug resistant *M. tb*

MTC − *Mycobacterium tuberculosis* complex

MTT − 3-(4,5-dimethylthiazol-2-yl)-2,5-diphenyltetrazolium bromide

MUG − 4-methylumbelliferyl beta-D-galactopyranoside

NAD and NADH − nicotinamide adenine dinucleotide

NADP and NADPH − nicotinamide adenine dinucleotide phosphate

NO − nitric oxide

NN – nitrate and nitrite

NPC – no phage control

NRP − non-replicating persistent state

PCR − polymerase chain reaction

PES − phenazine ethosulfate

pfu – plaque forming units

PGL − phenolic glycolipid

PZA – Pyrazinamide

qRT-PCR − quantitative real-time polymerase chain reaction

RD – region of difference

redox − reduction-oxidation

RIF – Rifampicin

SNP – single-nucleotide polymorphism

STPK − serine-threonine protein kinase

TB – tuberculosis

TCA cycle – tricarboxylic acid cycle

TCS – two-component system

TSS – transcription start site

XDR-TB − extensively drug resistant *M. tb*

CHAPTER 1: REVIEW OF THE LITERATURE

1.1 Tuberculosis: An Overview

1.1.1 Tuberculosis: A Global Problem

Tuberculosis (TB) is the earliest documented infectious disease (*1*), yet despite the availability of a vaccine and many targeted antibiotics it still remains one of the most important human pathogens. The major species responsible for TB is *Mycobacterium tuberculosis* (*M. tb*). Over one third of the world population is currently infected with *M. tb* (*2*). This accounts for 9.4 million new cases of TB and 1.7 million deaths due to TB every year (*2*). *M. tb* is the most common opportunistic infection in human immunodeficiency virus (HIV) infected individuals and is responsible for over a third of all acquired immune deficiency syndrome (AIDS) related deaths worldwide (*3*). This makes *M. tb* the single most deadly bacterial pathogen in the world.

M. tb has diverged into a number of genetically unique groups known as lineages. One of these lineages is the Beijing lineage. This lineage demonstrates a number of properties that may make it a more dangerous pathogen than other lineages of *M. tb*. One of the phenotypes associated with this lineage is the constitutive induction of the Dos regulon. This regulon is controlled by the DosR two-component system. This thesis focuses on identifying how genetic differences between different lineages of *M. tb* can affect expression and function of the DosR two-component system, which may ultimately explain the phenotype observed in Beijing strains. These results expand on our

knowledge of the DosR two-component system and its interacting partners. In the future this may help explain how strain variation affects pathogenesis of *M. tb*.

1.1.2 Milestones in the History of Tuberculosis

TB, historically referred to as consumption or phthisis, is the earliest documented infectious disease. There are fossil records of spinal TB dating from the Neolithic period (around 8000 BC) and non-viable bacteria have been extracted from a preserved Incan mummy from 700 BC (*1*). Hippocrates, known as the father of western medicine, described TB as the most common disease of his era (around 400 BC) (*1*). It is estimated that untreated TB has a mortality rate of over 50%, so it is apparent that TB was a major factor in population control in the pre-antibiotic era (*4*).

There are a number of important milestones in the study and treatment of TB. Before the discovery of *M. tb* there were many hypotheses for the cause of TB ranging from it being a hereditary condition to a form of cancer (*1*). In 1882 Robert Koch proved that an infectious agent caused TB. He was able to isolate *M. tb* from an infected host, culture it and use the preparation to infect a healthy host. This work became the basis for Koch's postulates, a set of criteria used to prove the causative relationship between a microbe and a disease. The first effective treatment for TB was the induction of a pneumothorax, or collapsed lung. This procedure was performed as early as 1888 and prevented transmission of the bacteria by preventing air flow to the infected portion of the lung (*1*). In the early 1900s, Dr. Calmette and Dr. Guérin developed the first vaccine for TB. This live attenuated vaccine, known as the BCG (bacilli Calmette-Guérin) vaccine, is still currently used worldwide. The next important milestone in TB treatment

was the development of the first anti-TB antibiotics. The first antibiotic discovered to be effective against *M. tb* was streptomycin, which was discovered in 1943 by Dr. Selman Waksman (*5*). This was followed by the introduction of Isoniazid (INH), Rifampicin (RIF), Pyrazinamide (PZA) and Ethambutol (ETB), which remain the mainstay of TB treatment today. In the modern age of genomics, perhaps the most important advance in TB research has been sequencing the *M. tb* genome. The first full genome sequence of a strain of *M. tb* was completed in 1998, which has since revolutionized the field of TB research (*6*).

1.2 Pathogenesis of *Mycobacterium tuberculosis*

1.2.1 Tuberculosis Disease

The major form of TB is pulmonary TB. Pulmonary TB is a chronic, destructive infection of the pulmonary tissue. TB disease is defined by the presence of granulomas, described in further detail below. In pulmonary TB, granulomas form and enlarge, destroying alveolar tissue required for respiration. Eventually the granuloma tissue will become necrotic and can liquefy. These granulomas are known as *caseating* granulomas. This will expose extracellular bacteria to the airways and lead to airway irritation. This causes the patient to develop a chronic cough that produces aerosols containing infectious bacteria. The patient also produces bloody sputum, loses weight and energy and can develop pneumonia. The rupture of large blood vessels in the lungs will eventually lead to suffocation and death (*7*).

M. tb can also replicate and cause pathogenesis outside of the lung (extrapulmonary TB). This is either due to dissemination of *M. tb* away from the lung through the circulatory or lymph system or may also result from *M. tb* infection through a non-pulmonary route of entry. The most common locations for extrapulmonary TB are the intestines, the central nervous system, bones and joints (*7*). Infected individuals can also have a fully disseminated form of TB known as miliary TB.

An important consideration for the global TB epidemic is the emergence of HIV in the human population. Co-infection with HIV and TB is a very serious and common problem. The major population reservoir for HIV and TB overlap so there are a lot of individuals who are co-infected. Of the 9.4 million new cases of TB every year, 1.4 million cases are in HIV-infected individuals (*8*). These diseases act synergistically, whereby the progression of both conditions is more rapid during co-infection. TB is the most common opportunistic infection in HIV infected individuals, who are 20 times more likely to develop TB then HIV-negative individuals (*9*).

1.2.2 Antibiotics

Since the advent of modern mycobacterial antibiotics, TB has transitioned from a deadly, debilitating disease into a treatable illness. However, there remain many limitations with anti-TB therapy. The first is the extended time course of antibiotics required to cure patients. The current treatment for active TB is a combination of drugs to prevent the development of antibiotic resistance. The usual course of treatment is the use of RIF, INH, ETB and PZA for two months followed by treatment with just RIF and INH for four months. This time course can even be extended to 12 months dependent on the

initial pathology and the adherence to treatment regime (*7*). The usual course of treatment for latent TB, a condition described in more detail below, is the use of only INH for six months and is effective in preventing reactivation of latent infection. As treatment periods are very long compared to most other diseases, compliance and antibiotic resistance are very severe problems for TB. In addition, the majority of TB cases present in the developing world, so drug supply is sometimes difficult to provide for the entire treatment regiment.

Like all other pathogens, *M. tb* has the ability to develop drug resistance. Multi-drug resistant *M. tb* (MDR-TB) and extensively drug resistant *M. tb* (XDR-TB) pose a great threat to *M. tb* treatment and containment (*10*). MDR-TB is resistant to both INH and RIF while XDR-TB is resistant to INH, RIF and some second line drugs like quinolones.

It also appears that even after antibiotic treatment and clearance of all M. tb, a strong immunological memory is not formed in the host. Therefore, patients can be reinfected with M. tb if they remain in an area with high transmission (11). Since M. tb can also persist in a host for long periods of time and spontaneously reactivate, elimination of M. tb is difficult. Latent carriers can spread TB to low-incidence areas through emigration. Therefore, the best-case scenario for the global TB epidemic is for the continued containment of TB until it slowly decreases in the population.

There are only a few drugs that effectively treat TB, so the spread of resistant strains poses worldwide health risks. Without effective drugs, TB could once again become an untreatable disease with high mortality. The most recently developed TB

drugs, such as INH and RIF, were created about 40 years ago (*12*). The genome and proteome of *M. tb* have revealed an abundance of potential antibiotic targets involved in virulence and homeostasis. Designing therapeutics specific for some of these novel targets may also be more effective at quickly eliminating *M. tb*. This could decrease the length of the drug regimen and increase the compliance of patients. If drugs specific for novel targets can be designed we may be able to control and contain the rising number of cases of MDR-TB and XDR-TB.

1.2.3 Vaccine

The current vaccine for TB is a live attenuated vaccine composed of a derivative of *Mycobacterium bovis* (*M. bovis*), known as the BCG vaccine. The BCG vaccine is one of the most widely used vaccines in the world, with over 3 billion people already vaccinated (*13*). The BCG vaccine has been used for nearly a century and is non-pathogenic for the majority of recipients. It was initially isolated by serial ex-vivo passaging of *Mycobacterium bovis* until virulence was lost. In endemic TB regions, the BCG vaccine is given at birth despite the fact that it appears to show variable efficacy depending on the age and geographical location of the recipient (*14*). Clinical trials show the effectiveness of the vaccine can range anywhere between 80% and 0% (*15*). A trial evaluating the efficacy of BCG was conducted between 1956 and 1963 on 54,239 school children in the United States who received the BCG vaccine when they were 14 or 15 years old. This study showed an efficacy of 84% up to 6 years after immunization (*16*). On the other hand, another BCG vaccine trial in the United States in 1966 showed an efficacy of only 14% (*17*). A trial in India in 1979 showed no protective effect of BCG

vaccination (*18*). Therefore new vaccine candidates and vaccination strategies are required for better prevention of TB.

1.2.4 Route of Infection

M. tb is spread predominantly through inhalation of infectious aerosols. When a patient with active pulmonary TB coughs or sneezes, they release a large cloud of microscopic droplets containing *M. tb*. Particles less than 10 microns in diameter can reach alveolar tissue if they are inhaled (*19*). The bacteria within these aerosols are then phagocytosed by alveolar macrophages. *M. tb* can survive and replicate within the phagosome of macrophages and can eventually spread to new macrophages and other immune cells. *M. tb* has a very low infectious dose. In controlled infection experiments, cattle could be infected and develop active disease after inhalation of as few as a single bacillus of *M. bovis* (*20*). It is estimated that 25% of individuals who inhale infectious aerosol particles will get infected with *M. tb* (Figure 1). Of these 25%, around 10% will go on to develop active disease, usually within a year of the initial infection. The rest develop a latent infection, whereby they show no pathology, however the bacteria are able to survive and persist for decades with little or no replication (*21*).

1.2.5 Cell Escape

The first stages of *M. tb* infection are relatively well known. Alveolar macrophages phagocytose *M. tb* bacilli. *M. tb* can survive in the phagosomes of macrophages by preventing phago-lysosomal fusion (*22*). The accepted paradigm of macrophage survival is that *M. tb* stays sequestered in the phagosome and multiplies,

eventually leading to death of the infected macrophage. Extracellular *M. tb* can then be phagocytosed by other macrophages, perpetuating the infection (*23*). Recently, new research has demonstrated that *M. tb* may be able to escape the phagosome, and then survive and proliferate in the cytosol of infected macrophages (*24*). These bacteria may even be able to transfer directly between macrophages by triggering the creation of a cellular junction by a process known as non-lytic ejection as has been described in the *Dictyostelium* amoeba model of macrophage infection (*25*).

Figure 1: Disease Progression for Tuberculosis
Individuals exposed to TB have approximately a 25% chance of being infected. Of those individuals, around 10% develop active TB within the first year of infection. The remaining 90% develop a latent infection. Over the remainder of their lifetime, 5-10% of latently infected individuals will develop active TB due to reactivation of latent *M. tb*.

1.2.6 Granulomas

TB pathology is defined by the presence of granulomas, also known as tubercules. A granuloma is an aggregate of the host's immune cells that act to isolate *M. tb* bacilli from uninfected cells. A normal granuloma has a center of infected macrophages surrounded by healthy macrophages, T cells and B cells (Figure 2). The core of infected macrophages can begin fusing together and create multinucleated giant cells (*26*). It was always assumed that the formation of the granuloma was a host response to infection that

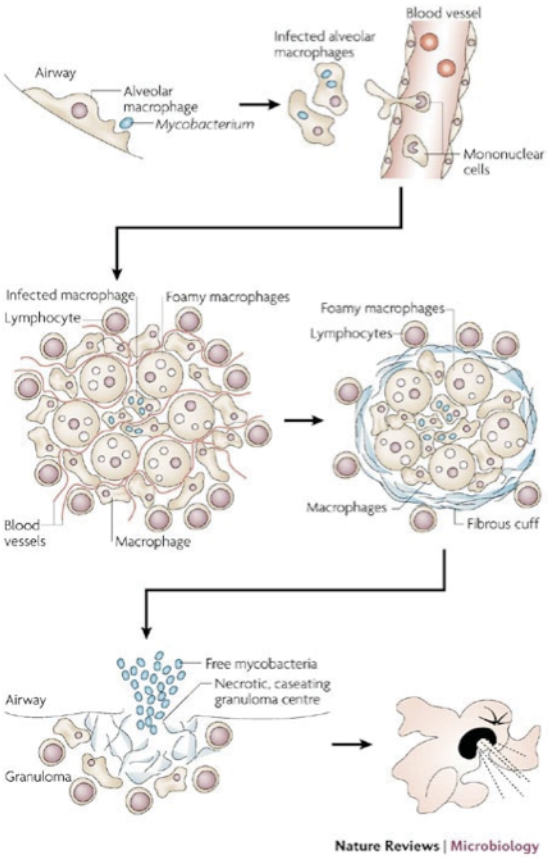

Figure 2: Macrophage Infection and Granuloma Formation
Alveolar macrophages phagocytose inhaled *M. tb*.. A localized immune response recruits uninfected macrophages and other immune cells to the site of infection. The immune cells organize around the infection site and the site eventually becomes walled off. There is a central core of infected macrophages and giant cells surrounded by a layer of collagen and extracellular matrix, which is in turn surrounded by a layer of T-lymphocytes. Under favourable conditions, the granuloma can become necrotic and bacterial replication will resume. *M. tb* can then gain access to the airways and will be able to infect new hosts, thus restarting the infection cycle. From: Russell, D.G., Who puts the tubercle in tuberculosis? Nat. Rev. Microbiol., 2007. 5: p. 39-47, with permission.

served to inhibit and contain the spread of *M. tb* in the host (*22, 23, 27*). Recent work using live imaging of cell traffic in granulomas indicates this may not be entirely correct. Using the zebrafish embryo model of TB infection, research indicates that there is active egress of *M. marinum*, a closely related Mycobacteria, infected cells from granulomas to other tissues (*28, 29*). This process may also be occurring with *M. tb* in human granulomas. Other data reveals that here also appears to be very high conservation in the T-cell epitopes of *M. tb* (*30*). This indicates that there is an evolutionary benefit for T-cell recognition of *M. tb* and further indicates that *M. tb* profits from host recognition and the formation of a granuloma. *M. tb* could benefit from granuloma formation because uninfected macrophages are recruited to the site of *M. tb* infection. This provides a

constant source of uninfected cells to allow for *M. tb* multiplication and dissemination. Whichever paradigm is correct in human infections, the granuloma represents a state of equilibrium between infectious agent and host response. As mentioned previously, the majority of infected individuals do not develop active disease. Concomitantly, the majority of granulomas can persist for long periods of time without expansion or tissue destruction. When this balance is disrupted, the granuloma expands and the host cells undergo necrosis. This leads to a large amount of extracellular bacteria, tissue destruction, host transmissibility and mortality.

1.2.7 Latency and Non-Replicating Persistence

Latency is one of the defining features of TB disease. The ability of *M. tb* to persist in hosts without causing pathology is one of the major reasons it remains such a prominent pathogen. Latency results in a large reservoir of individuals who can spread disease and who will likely not be treated themselves (*31*). 5%-10% of infected individuals with latent TB will "reactivate" and develop active TB decades after their initial infection (*32*). This also allows for the spread and dissemination of TB as asymptomatic carriers can emigrate from their native country and reactivate in another population where *M. tb* is not as prevalent.

The exact state of *M. tb* during latency is debated. It is generally agreed that *M. tb* undergoes a metabolic shift that allows it to become less active and less immunoreactive (*33*). This is often called the latent state, dormant state, persistent state or non-replicating persistent state (NRP). These bacteria in NRP are resistant to antibiotics that affect actively replicating bacteria and are normally non-cultivable on media (*33*). These

bacteria are very hardy and have been shown to survive for as long as 12 years in sealed liquid culture (*34*).

The concept of NRP is an integral part of *M. tb* pathogenesis, it affects both the treatment and dissemination of *M. tb* and needs to be understood in order to treat and contain disease. Consequently, there have been vast amounts of research attempting to understand the mechanisms behind the adaptation of *M. tb* to NRP. It is thought that latent *M. tb* can survive despite being surrounded by a granuloma. The environment of a granuloma is very hostile to the bacteria. There is no blood circulation, so the inside of a granuloma is hypoxic. Nutrients are also scarce, the pH can be very acidic and immune cells also produce nitric oxide (NO) (*35*). Researchers have attempted to reproduce this NRP state *in vitro* using a variety of models. One of the major ways that researchers attempt to induce NRP is by the induction of hypoxia. It has been observed that *M. tb* granulomas appear to localize to regions of high oxygen concentration. For example, reactivation of *M. tb* in humans occurs predominantly in the upper lobes of the lung, while reactivation of *M. bovis* or *M. tb* in cattle and rabbits occurs most often in the dorsal portion of the lungs (*35*). Both of these locations have the highest concentration of oxygen in the host. Conversely, limiting oxygen availability appears to limit *M. tb* growth. Pneumothorax induction helps control *M. tb* growth and even moving to a geographical area with an elevation in height and the associated decrease in oxygen tension can decrease transmission and disease progression (*36*).

A number of models have been developed using hypoxia to attempt to induce NRP *in vitro*. One such *in vitro* model is the Wayne model. In the Wayne model, *M. tb* cultures are put in a sealed tube with a defined headspace ratio. The bacteria are then

incubated with gentle stirring. The bacteria slowly consume all available oxygen, leading to a slow induction of hypoxia (*37*). Another important model is the defined hypoxia model. In this model liquid cultures are placed in a microaerophilic environment, usually <1% oxygen, for the duration of their growth (*38*).

1.3 *Mycobacterium tuberculosis:* The Organism

1.3.1 The *Mycobacterium tuberculosis* Complex

TB is caused by a collection of genetically similar organisms known collectively as the *Mycobacterium tuberculosis* complex (MTC). These bacteria all have identical 16s RNA and share 99.9% conserved nucleotide similarity (*39*). The MTC appear to come from a common ancestor and are closely linked on a phylogenetic tree (Figure 3). These organisms can vary immensely in their host tropism and pathogenicity, although some members of the MTC share overlapping host organisms. The members of the MTC that can cause disease in humans are *M. tb*, *M. bovis*, *M. africanum* and *M. canetti*. These species are all closely related and vary by only a few deletions and mutations. *M. bovis*, initially described as the major cause of TB in cows, was once a major source of TB in humans, predominantly through contaminated milk. *M. bovis* was once implicated in as much as 30% of all cases of TB, but this has decreased drastically since the introduction of milk pasteurization (*1*).

The major human pathogen in the MTC is *M. tb*, therefore for the remainder of this thesis I will be focusing on *M. tb.* The *M. tb* genome is 4.4 megabases and codes for 3,959 unique genes (*6*). *M. tb* is a pathogen with many characteristics that render it

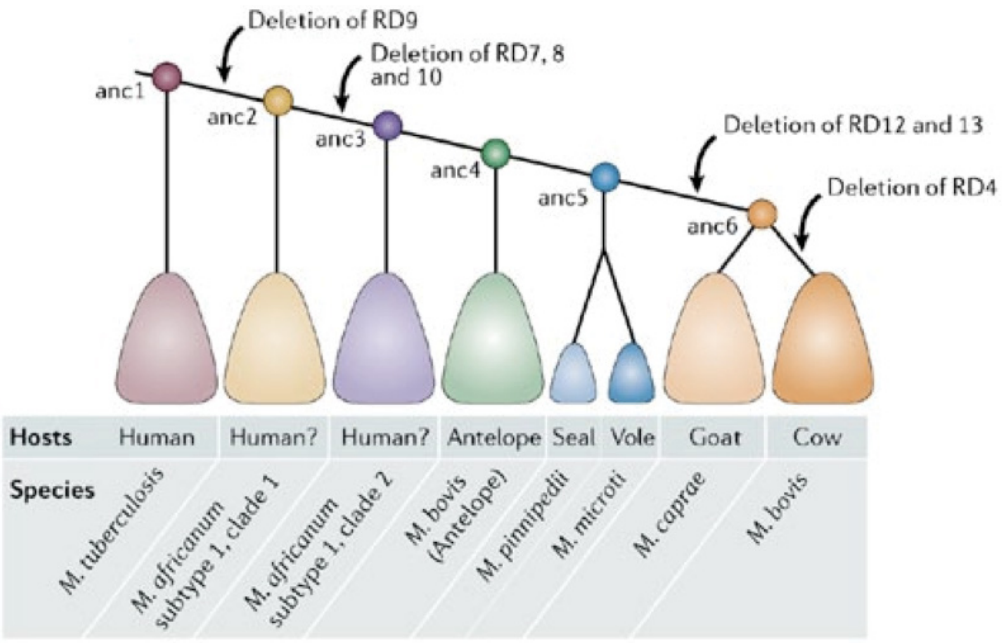

Figure 3: Phylogeny of the *Mycobacterium tuberculosis* Complex (MTC)
This phylogeny was based on genomic deletions and SNPs. The member of the MTC and the host tropism are indicated below. Anc1-anc6 represent a common ancestral strain for each member of the MTC. All animal-adapted strains contain the RD9 deletion. From: Smith, N.H. et al., *Bottlenecks and broomsticks: the molecular evolution of Mycobacterium bovis.* Nat Rev Micro, 2006. **4**(9): p. 670-681, with permission.

unique compared to many other bacteria. Certain aspects of the microbial physiology of *M. tb* and related mycobacteria, specifically its cell wall composition and metabolic pathways, are unique to this genus. *M. tb* is also adapted for long-term survival in its host, and as such is adapted to the development of long-term persistence within the host. All of these aspects are important to understand how *M. tb* causes disease and why it is such an incredibly successful pathogen

1.3.2 The Cell Envelope of *Mycobacterium tuberculosis*

Mycobacteria have a very unique cell envelope compared to other bacteria. *M. tb* is a bacillary bacteria and its cell envelope has a very high lipid content which renders it

unclassifiable by Gram staining. Therefore, identification of *M. tb* is normally performed using Ziehl–Neelsen staining. Regardless, *M. tb* is still classified as a gram-positive organism because it only has one cell membrane in its envelope resembles other gram-positive organisms, such as Streptomyces (Figure 4).

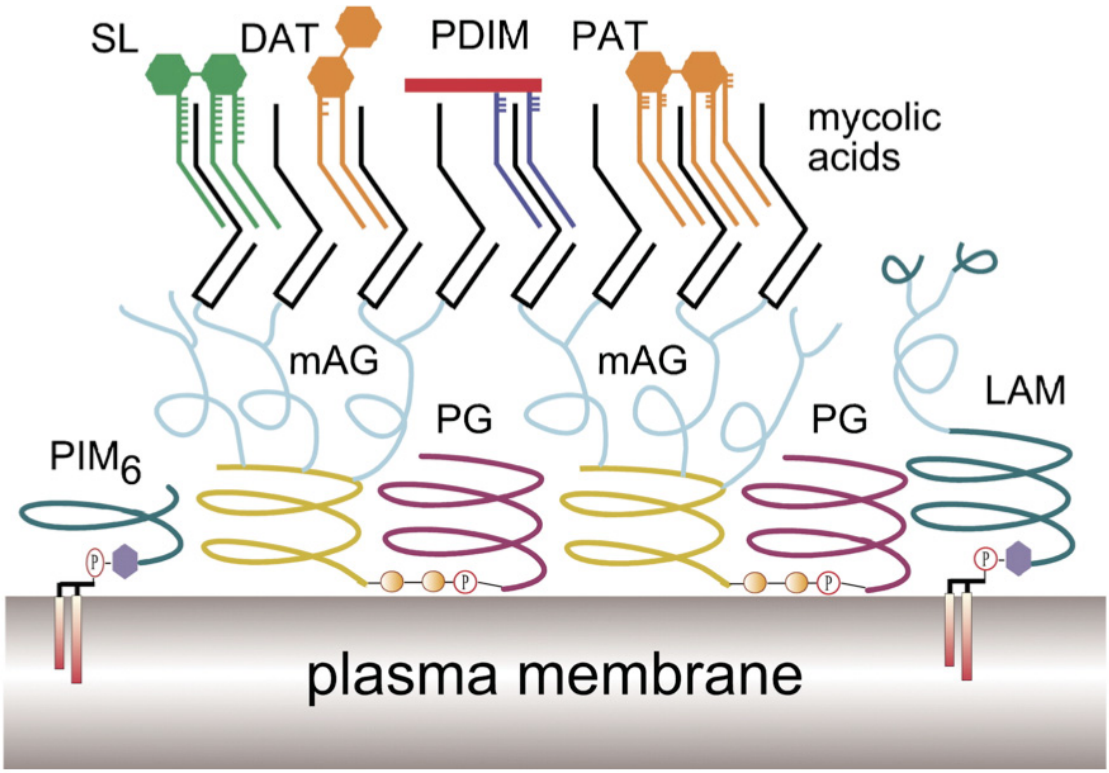

Figure 4 : Cell Wall Composition of *Mycobacterium tuberculosis*

Schematic depicting the cell wall of *M. tb*. PG: peptidoglycan, mAG: mycolyl arabinogalactan, PIM_6: phosphatidylinositol pentamannoside, LAM: lipoarabinomannan, SL: sulfolipid, DAT: diacyl trehalose, PDIM: phthiocerol dimycocerosate, PAT: pentaacyl trehalose. From: Minnikin, D.E., et al., *The Methyl-Branched Fortifications of Mycobacterium tuberculosis.* Chem. Biol., 2002. **9**(5): p. 545-553, with permission.

Approximately 60% of the dry weight of the cell envelope is composed of mycolic acids (*40*). The high lipid content of the membrane renders it highly hydrophobic and very impermeable. This appears to account for the resistance of *M. tb* towards antibiotics and chemotherapeutic agents (*41*). The presence of mycolic acids also contributes to the

resistance of *M. tb* towards dehydration and allows it to survive and persist in hostile environments like the macrophage (*42*). *M. tb* contains many other lipids that are physiologically relevant. Approximately 10% of its entire genome is dedicated to lipid metabolism (*6*). The genome codes for more than 250 different enzymes that are involved in fatty acid metabolism. In contrast, *Escherichia coli* (*E. coli*) only has 50 genes involved in lipid metabolism (*6*). Besides structural lipids, *M. tb* also encodes a variety of lipids that act as virulence factors. These include; trehalose dimycolate, lipoarabinomannan, sulfolipid, phthiocerol dimycocerosate and phenolic glycolipid (PGL) (*43-47*).

1.3.3 Central Carbon Metabolism in *Mycobacterium tuberculosis*

Central carbon metabolism (CCM) is a collective term that encompasses all metabolic processes associated with glycolysis, gluconeogenesis, the pentose phosphate shunt and the tricarboxylic acid (TCA) cycle (*48*). These metabolic pathways are found conserved in all organisms from bacteria to mammals, therefore little research has been invested in describing these pathways in individual organisms. It is assumed that these pathways have homologous carbon flux and regulation compared to the organism in which they were initially described, *E. coli*. It is becoming clear that this is not entirely true. *E. coli* and *M. tb,* for example, have very different ecological niches and survival strategies, so variation in carbon utilization pathways is understandable. *E. coli* has adapted its metabolism to focus on continuous, maximal cell growth. In contrast, *M. tb* alters between a state of active replication when it initially infects a host and a state of persistence, where there is no cell replication and has reduced ATP pools (*48*). *M. tb* also

uses lipids instead of simple sugars as its major carbon source during chronic infections (*49*). This difference in metabolism is mirrored in cell growth rates. *E. coli* has a cell doubling time of ~20 minutes while *M. tb* has an estimated doubling time of ~24 hours.

It is only recently that differential metabolism through the CCM has been examined in *M. tb*. Genes involved in CCM in *M. tb* were shown to be involved in cell survival in an *in vivo* infection model (*50*). This indicates that CCM enzymes may serve both physiological and pathogenic roles in *M. tb*. Transcriptional profiling has also demonstrated that there are large changes in expression of CCM genes in *M. tb* following infection of macrophages, mice and humans (*51, 52*). *M. tb* has many functionally redundant enzymes in CCM. Many of these enzymes have overlapping functions with only small changes in substrate specificity (*48*). This allows *M. tb* to co-metabolize multiple carbon sources simultaneously and even in opposite directions, a process that *E. coli* can not perform (*53*). *M. tb* also has a discontinuous TCA cycle, impaired gluconeogenesis and many novel metabolic reactions and regulatory controls (*48*). Therefore, CCM in *M. tb* differs from many other bacteria, it has unknown regulation and functions and is implicated in the pathogenesis of *M. tb*.

1.3.4 The Dormancy Survival Regulon

The ability to undergo NRP is one of the major reasons *M. tb* is such a successful and widespread pathogen. In order to understand the intracellular changes occurring in *M. tb* during NRP, transcriptional changes were assessed in cultures that underwent growth in both the Wayne model and the defined hypoxia model, described in section 1.2.7. Microarray data identified a set of 48 genes that appeared to be very quickly induced after

hypoxia (*54*). These genes were also shown to be induced by the presence of Diethylene triamine/nitric oxide (DETA/NO), a NO donor (Figure 5). This set of genes was labeled the dormancy survival regulon, or Dos regulon. The majority of these genes do not have any predicted function, but some genes are involved in alternative electron transport and anaerobic metabolism, processes that would be important during NRP.

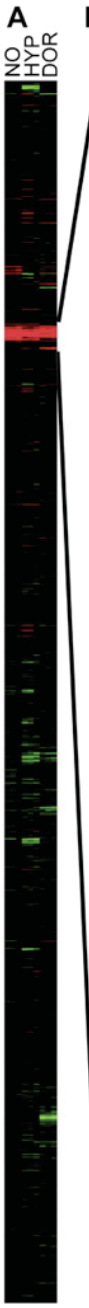

B

Rv No.	Gene	NO	HYP	DOR	Protein Function
79		15	13	16	HP
80		6	8.2	11.1	HP
81		2.8	3.8	7.2	Transcriptional regulator
569		24	17	9	CHP
570	*nrdZ*	3	3.0	8.3	Ribonucleotide red.cl. II
571c		4.3	1.8	2.5	CHP
572c		17	9.4	6.7	HP
573c		1.9	1.3	1.0	CHP
574c		4.9	2.9	5.0	CHP
1733c		21	16	6	CHP
1734c		5.7	5.1	1.9	HP
1735c		1.9	2.0	1.8	CHP
1736c	*narX*	4	3.3	8.1	Fused nitrate reductase
1737c	*narK2*	15	13	5	Nitrite extrusion protein
1738		27	50	24	CHP
1812c		2.4	2.0	7.8	HP
1813c		18	13	22	HP
1996		15	14	5	CHP-USPA motif
1997	*ctpF*	7	4.4	9.4	Cation transport ATPase
1998c		16	8.6	1.8	CHP
2003c		14	12	6	CHP
2004c		2	2.1	8.0	HP
2005c		7	9.2	11.1	CHP-USPA motif
2006	*otsB1*	4.1	4.0	2.6	Trehalose phosphatase
2007c	*fdxA*	16	24	18	Ferredoxin
2028c		4.8	3.5	17.3	CHP-USPA motif
2029c	*pfkB*	16	12	23	Phosphofructokinase II
2030c		19	11	48	CHP
2031c	*acr*	23	15	31	α-Crystallin
2032	*acg*	31	45	24	CHP
2623		6	7.3	27.3	CHP-USPA motif
2624c		17	20	5	CHP-USPA motif
2625c		5.6	6.9	5.3	CHP
2626c		15	41	57	CHP
2627c		11	12	15	CHP
2628		8	5.2	23.1	HP
2629		7.2	7.4	7.7	HP
2630		5	4.2	16.2	HP
2631		2.0	1.6	6.2	HP
3126c		22	23	2	HP
3127		25	36	21	CHP
3128c		12	18	2	CHP
3129		26	25	3	CHP
3130c		21	14	28	CHP
3131		5	4.6	40.4	CHP
3132c		12	9.8	12.7	Sensor histidine kinase
3133c	*dosR*	14	12	12	2-comp. response reg.
3134c		9	11	23	CHP-USPA motif

Figure 5: The Dormancy Survival Regulon

Identification of all members of the Dos regulon by microarray analysis. **A)** Microarray analysis examining *M. tb* gene transcription under three conditions compared to untreated controls: NO: 40' exposure to 50μM of NO donor DETA/NO. HYP: Defined hypoxia model, exposure to 0.2% O_2 for 2h. DOR: Wayne model after 4 days. Red indicates induced, Green indicates repressed and black indicates no change. **B)** List of all Dos regulon genes identified by microarray analysis. Arrows represent co-transcribed operons. HP: Hypothetical protein. CHP: Conserved hypothetical protein. From: Voskuil, M.I., et al., Inhibition of Respiration by Nitric Oxide Induces a *Mycobacterium tuberculosis* Dormancy Program. J. Exp. Med., 2003. **198**(5): p. 705-713.

Another gene, *hspX*, codes for α-crystalin homologue protein and is both an antigen and a chaperone protein. It is induced up to 80 fold upon regulon induction (*55*). The Dos regulon is also induced during infection of macrophages, mice and guinea pigs and in standing cultures (*M. tb* settles to the bottom creating a hypoxia gradient) (*56-58*). It is also induced by carbon monoxide (*59-61*).

The Dos regulon is induced very quickly after induction of hypoxia. Significant transcription of regulon genes is seen by 4 hours. High induction is seen for all genes by 12 hours and by 24 hours transcription of about half the regulon returns to baseline, although some genes do remain significantly upregulated for the duration of hypoxia. (*38*). Therefore, it seems that the Dos regulon is predominantly transiently expressed and is involved in the early response of *M. tb* to the macrophage environment.

There is also evidence to suggest that the Dos regulon may be involved in the recovery of M. tb from NRP back to a state of active replication. When induction of the regulon is ablated, *M. tb* recovers back to a state of active replication from NRP slower and has decreased viability compared to the parental strain (*62*).

1.3.5 Enduring Hypoxic Response

It appears the Dos regulon is not the only set of genes to be induced by hypoxia. By following longer time courses after establishment of hypoxia, a set of 230 genes independent of the Dos regulon were found to respond (*38*). In contrast to the Dos regulon, these genes were not induced early after hypoxia. Rather, they were induced between 4 to 7 days after establishment of hypoxia (*35*) (Figure 6). These genes were

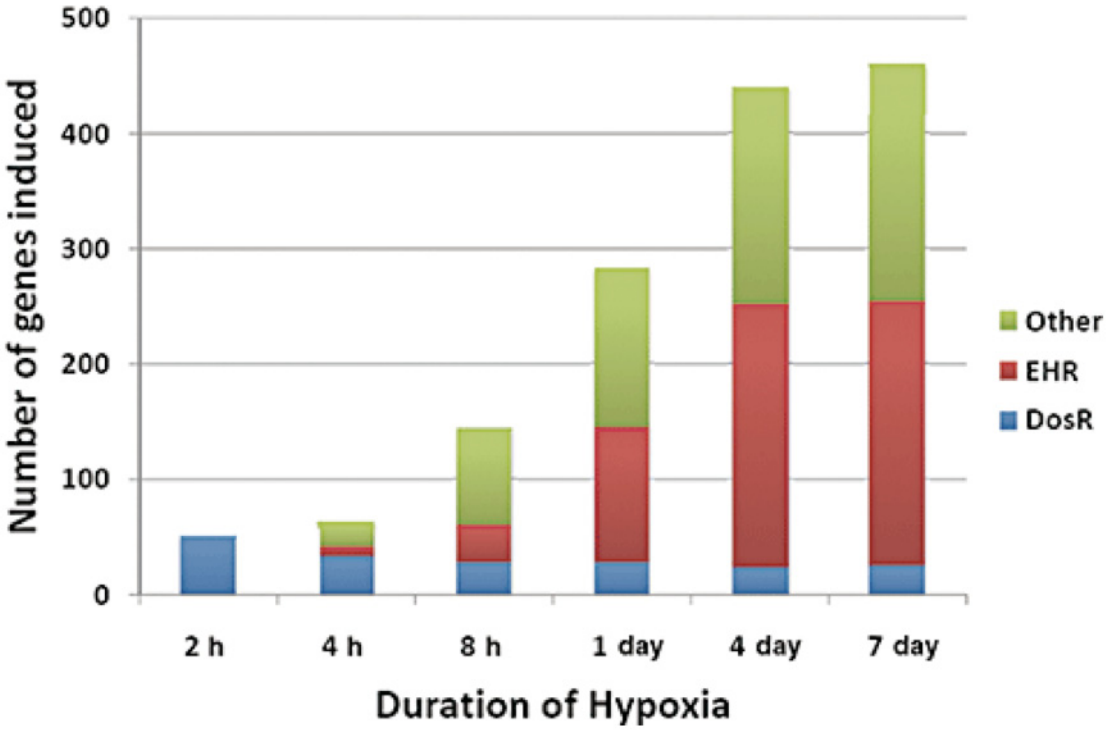

Figure 6: Expression of Dos Regulon and Enduring Hypoxic Response Genes Bar graph depicts *M. tb* gene expression during the defined hypoxia model. The y-axis represents total number of genes induced. The x-axis represents duration of time cultures experienced hypoxia. EHR: enduring hypoxic response operon genes. DosR: Dos operon genes. From: Rustad T.R. et al., *Hypoxia: A window into Mycobacterium tuberculosis* latency. Cell Microbiol, 2009. **11**(8): p. 1151-1159, with permission.

designated the Enduring Hypoxic Response (EHR). Within the EHR there are a large number of putative transcription factors as well as genes potentially involved in anaerobic respiration (*38*). It also appears that induction of the EHR is independent of any genes in the Dos regulon or the transcription factor responsible for Dos regulon induction, DosR (described in more detail below). Ablation of the *dosR* locus does not affect induction of EHR genes (*35*). These results implicate the Dos regulon in surviving the initial exposure to hypoxia or NO within the macrophage, and preparing the bacteria for the development of the NRP phenotype (*38*).

1.4 Phylogenetics and Lineage Variability

1.4.1 Mutations and Divergent Lineages

M. tb has unique genomic properties that have lead to the development of distinct divergent lineages (*63*). The three major forms of mutation in bacteria are horizontal gene transfer (HGT), single base pair mutations and indels (genomic insertions or deletions).

HGT is not a major factor in the evolution and divergence of different lineages of *M. tb*. It is thought that the common ancestor of the MTC was once an environmental organism that was able to undergo HGT with other organisms (*14*). The current members of the MTC are all obligate pathogens, so they are rarely found in an environment with other bacteria where they can undergo HGT (*15*).

The rate of point mutations in *M. tb* is much lower than many other related bacteria (*64*). This allows for differentiation of divergent strains based on a small pool of single-nucleotide polymorphisms (SNPs). Although, recent publications have examined the functional diversity between different strains of TB and they appear to suggest that SNPs may have a larger impact on gene expression in *M. tb* then previously thought (*65*). Some labs have begun sequencing multiple strains from many lineages to get a comprehensive understanding on SNPs between different lineages (*66*).

Large genomic duplications and deletions are a major form of mutation separating divergent lineages of *M. tb*. The environmental ancestor of *M. tb* required many more genes for survival outside of a host. As the current members of the MTC have specific niches they appear to no longer require many of these genes. Therefore, they have

undergone a process termed reductive evolution, wherein they spontaneously loose large genomic regions that are unnecessary or interfere with survival in their new environments (*67*). The deletions are known as large sequence polymorphisms (LSPs) or regions of difference (RDs). These deletions have occurred independently in different divergent strains of *M. tb* and can be used to divide *M. tb* into different lineages (Figure 7). *M. tb* can be subdivided into six different lineages; Indo-Oceanic, Beijing (or East-Asian), East-African/Indian, Euro-American, West-African 1 and West-African 2. West-African 1 and West-African 2 lineages are both subspecies of *M. africanum*. Phylogenies of *M. tb* strains based on either divergence of RDs or SNPs are in high concordance, demonstrating that both techniques can measure genetic divergence (*68*).

1.4.2 Lineage Distribution

The different lineages of *M. tb* are predominantly found in different geographic locations (*69, 70*). As mentioned previously, *M. tb* has been a human pathogen since the Neolithic era. Consequently, *M. tb* has spread and diverged with the propagation and migration of the human species. This has lead to co-evolution of different lineages with different endemic populations. Consequently, specific populations may be more or less susceptible to specific strains of *M. tb*. With the advent of fast affordable worldwide transportation, *M. tb* lineages can be readily transported to new populations worldwide. Some of these lineages may have unique physiological characteristics that can allow for easy dissemination and pathogenesis in these foreign, unadapted populations.

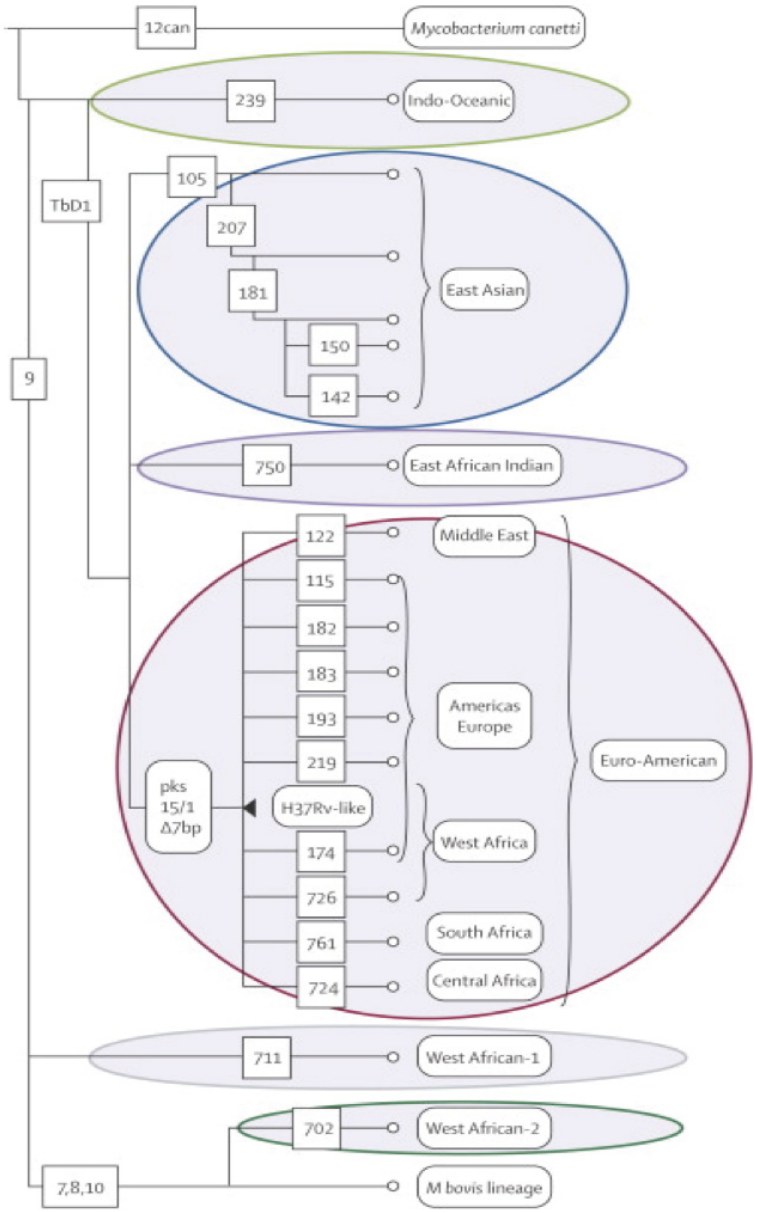

Figure 7: Phylogeny of *Mycobacterium tuberculosis* Lineages
Phylogenetic tree showing separation of *M. tb* into separate lineages based on LSPs. Identity of LSPs depicted in rectangles. Ancestral Beijing strains are represented by the group with the RD105 deletion but not RD207 deletion. Modern Beijing strains are represented by the groups with the RD105 deletion and the RD207 deletion. Light green oval: Indo-oceanic lineage, Blue oval: Beijing lineage, Purple oval: East Africa lineage, Red oval: Euro-American lineage, Grey oval: West African 1 lineage, Dark green oval: West African 2 lineage, pks: polyketide synthase gene. From: Gagneux, S., et al., *Global phylogeography of Mycobacterium tuberculosis and implications for tuberculosis product development*. Lancet Infect. Dis., 2007. **7**(5): p. 328- 337.

1.4.3 The Beijing Lineage

The East-Asian lineage, also known as the Beijing lineage, was initially described as the prevalent genotype of *M. tb* in East Asia. This lineage is subdivided into five separate groups, differentiated by genomic deletions (Figure 7). For the purpose of this thesis, group 1 Beijing strains will be referred to as ancestral Beijing strains while groups 2-5 will be referred to as modern Beijing strains. Recent research indicates the Beijing lineage has a selective advantage over other lineages of *M. tb*. This is supported by epidemiological, immunological, pathological and phenotypic data.

Epidemiological data indicates that the Beijing linage accounts for 50% of all TB cases in East Asia and 13% of all cases of TB worldwide (*71*). In addition, it appears that the total proportion of TB cases caused by the Beijing lineage is increasing in many geographic locations. For example, over a 12 year study in Cape Town, South Africa, the incidence rate for the majority of all lineages remained relatively stable, but the incidence rate for the Beijing lineage increased exponentially over time, with a doubling time of 4.86 years (*72*). This trend is also apparent in many other geographic locations including Russia, South Africa, Cuba, Bangladesh and Western Europe (*73*). It also appears that the BCG vaccine may be less protective against the Beijing lineage compared to other strains. In a recent meta-analysis, strains from the Beijing lineage were shown to be responsible for disease more often than other strains in individuals vaccinated with BCG (*74*). This indicates that individuals vaccinated with BCG may be more susceptible to Beijing strains. Likewise, BCG vaccination was less protective against Beijing strains in both mouse and rabbit models (*75, 76*) Beijing strains may also be more prone to

developing antibiotic resistance. In some locations, there is an enrichment in the proportion of antibiotic resistant strains from the Beijing linage (*77*). This may be associated with an increased mutation rate in antibiotic resistance genes (*78, 79*).

The Beijing lineage appears to also elicit a different immune response compared to other lineages. In one study, Beijing strains preferentially induce humoral immunity as opposed to cell-mediated immunity (*80*). Since *M. tb* is an intracellular pathogen, this may confer a survival advantage to Beijing strains compared to other lineages. In an *in vitro* macrophage infection assay, HN878, a Beijing strain, preferentially induced IL-4 and IL-13 which lead to Th2 polarized immunity. Infection with CDC1551, a non-Beijing strain, caused the induction of IL-12 and other molecules that lead to the development of Th1 protective immunity (*80*). Certain polymorphisms in human immune response proteins are also associated with infection with the Beijing lineage. Polymorphisms in both TLR2 and NRAMP1, two loci known to be important in sensing and responding to mycobacteria, were shown to be associated with increased vulnerability to strains from the Beijing lineage within one Vietnamese study (*81, 82*).

The Beijing lineage is also unique from a pathological perspective. When macrophages die by necrosis, the plasma membrane of the macrophages is ruptured and *M. tb* can escape from the lysed cell and infect other macrophages. In apoptosis, the cell membrane remains intact and *M. tb* shows decreased viability (*83*). In THP-1 macrophages, a Beijing strain caused a higher proportion of necrosis to apoptosis compared to a non-Beijing strain (*84*). This may allow Beijing strains to preferentially spread and infect macrophages compared to non-Beijing strains.

In mouse and rabbit models, the Beijing lineage caused more severe histopathology, higher bacterial burdens and higher mortality (*85, 86*). The propensity to develop disseminated disease also varied by strain background. A higher proportion of Beijing to non-Beijing strains lead to extrapulmonary TB (*87*). Another interesting study indicates that the rate of progression from the time of infection to active disease is shorter in patients infected with strains from the Beijing lineage (*88*).

Different strains of *M. tb* display different *in vivo* and *ex vivo* survival. The first targets of *M. tb* in humans are alveolar macrophages. In an *ex vivo* infection of THP-1 cells, a model for macrophage infection, there were significant differences in intracellular growth between some Beijing strains and non-Beijing strains, although there was significant variation in growth rate within the Beijing lineage as well (*89*). In an *in vivo* murine model, expression of PGL, a lipid expressed in certain strains in the Beijing lineage, was found to be associated with hyperlethality (*47*). In addition, Beijing strains appear to constitutively overexpress triglycerides, an important carbon source, which may help in survival during NRP (*73*). As described below, Beijing strains also appear to overexpress a number of proteins including the virulence factor α-crystalin protein homologue and the transcription factor DosR (*73, 90*).

1.5 The DosR Two-Component System of *Mycobacterium tuberculosis*

1.5.1 Two-Component Systems

Two component systems (TCSs) are ubiquitous signaling systems found predominantly in bacteria, but have homologues in all organisms. In their simplest form

they consist of a sensor kinase protein and a response regulator protein. The sensor kinase protein is composed of two domains, a sensor domain and a kinase domain. Sensor kinases are often embedded in the cell membrane. The response regulator protein normally has three domains; a N-terminal activation domain, a central linker region and a C-terminal effector domain. When its cognate signal is present, the sensor domain of the sensor kinase will undergo a conformation change, which leads to activation of the kinase domain. The activated kinase domain will then auto-phosphorylate at a conserved histidine residue. The phosphorylated sensor kinase can then transfer a phosphoryl group to a conserved aspartate on the activation domain of the response regulator (*91*). This activated response regulator can then perform a biochemical action, e.g. DNA binding, protein binding or activate enzymatic activity (*92*). The most common type of response regulator has a DNA binding domain for its effector domain. These proteins bind DNA and recruit an RNA polymerase to induce RNA transcription. There are three subfamilies of DNA binding domains in bacteria based on their sequence identity; NarL-like, OmpR-like and NtrC-like (*93*).

1.5.2 Regulation of Two-Component Systems

There are many variations of the basic two-component system and many levels of potential regulation. Some TCSs have multiple sensor kinases or response regulators (*91*). Some systems, known as three-component systems or phosphorelays, have an intermediate or adaptor protein required for the interaction of the sensor kinase and response regulator (*94*). These adaptor proteins are very important because their transcription is often induced by different regulatory stimuli (*91*).

There are also examples of bacterial proteins that block autophosphorylation of sensor kinases (*95*). Some proteins can promote the dephosphorylation of the response regulator protein or adaptor proteins (*96, 97*). Some proteins will block the dephosphorylation of a response regulator, leading to constitutive activation of the system (*98*). There are also some proteins that can activate sensor kinases even when stimuli are not present (*99*).

In the case of response regulators that are transcriptional activators, some regulatory proteins will directly bind the response regulator and inhibit oligomerization or DNA binding (*100*). Other regulatory protein can interfere with the association between a response regulator and recruitment of an RNA polymerase, inhibiting transcription (*101*).

A final potential level of regulation is either the inhibition or recruitment of proteases to components of the two-component system (*102*). Therefore, there are many different potential levels of regulation in such a seemingly simple signal transduction system. An alteration in either production or activity of any one of these regulatory proteins could lead to either inhibition or constitutive activation of signaling through their cognate response regulators.

1.5.3 Two-component Systems in *M. tuberculosis*

M. tb has a large variety of systems to sense and respond to changes in its environment. The three major types of regulatory systems are serine-threonine protein kinase (STPK) cascades, TCSs, and extracytoplasmic sigma factors. *M. tb* has 11 putative STPKs and 12 putative TCSs along with 5 orphan TCS components (*103, 104*). These

regulatory systems have overlapping induction stimuli and downstream effects. There is even an example of crosstalk between a STPKs and a TCSs (*105*). The components of *M. tb* TCSs are often found adjacent to one another in the genome and are coexpressed. Five of the twelve TCS in *M. tb* are conserved in all mycobacteria except *M. leprae*; PhoP-PhoR, KdpD-KdpE, TrcR-TrcS, DosR-DosS, and TrcX-TrcY (*104*). These TCS are thought to be the minimum number of TCSs required for mycobacteria.

1.5.4 The DosR Two-Component System

The regulation of the Dos regulon, described in section 1.2.7, has been demonstrated to be dependent on the DosR TCS. This TCS is composed of one response regulator and two cognate sensor kinases (Figure 8). The DosR TCS was initially described in 2000 as a putative virulence mechanism because it was overexpressed in a virulent *M. tb* strain, H37Rv, compared to an avirulent strain, H37Ra (*106*). DosR and one of its cognate sensor kinases, DosS, are cotranscribed as an operon (*106*). The other cognate sensor kinase, DosT, was originally an orphan sensor kinase and its relationship with DosR was only elucidated in 2004 (*107*). DosR and DosS are themselves both members of the Dos regulon. DosR TCS signaling was initially implicated in Dos regulon signaling due to their similar induction conditions (*108*). Ablation of the operon coding for DosR and DosS eliminated the induction of the Dos regulon, verifying that DosR TCS signaling is required for the hypoxic induction of the Dos regulon (*109*).

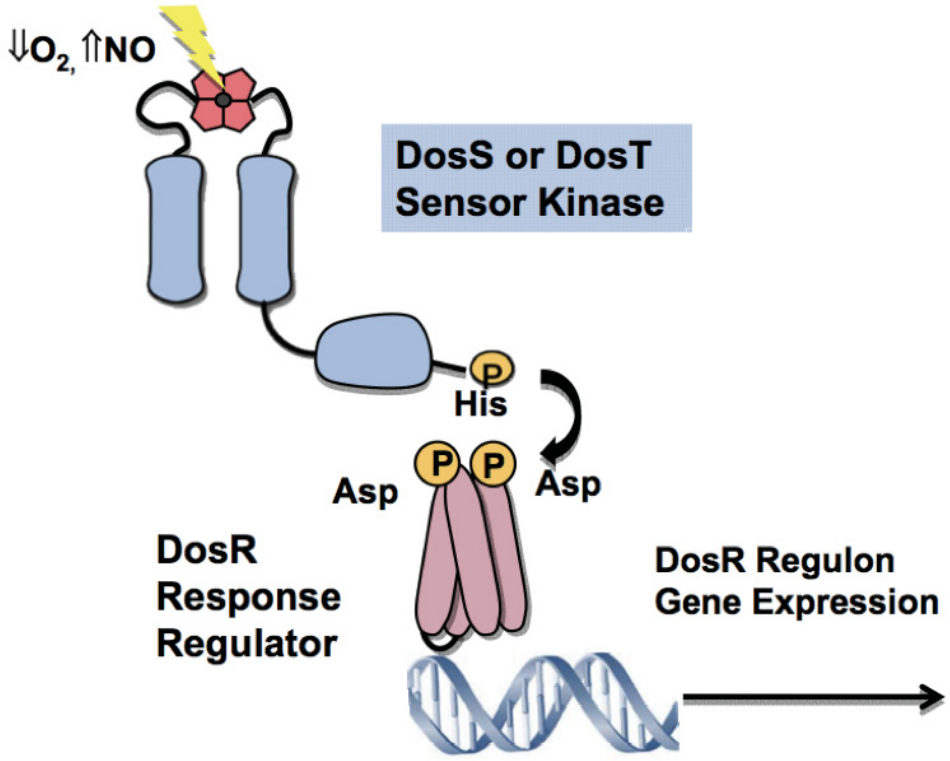

Figure 8: Schematic of DosR Two-Component Signaling
This diagram depicts the basics of DosR two-component signaling. Upon sensing an environmental stimuli like hypoxia or NO, DosS or DosT undergo auto-phosphorylation at a conserved histidine site. DosS and DosT can then phophorylate the DosR response regulator at a conserved aspartic acid residue. DosR can then oligomerize and bind to DosR boxes in the promoter region of DosR regulon genes. NO: Nitric oxide, Asp: Aspartic acid residue, His: Histidine residue, P: Phosphoryl group. Figure kindly provided by A. Fallow, M.Sc. Thesis 2009.

1.5.5 The Mechanism of DosS and DosT Activity

DosT and DosS are both homologous sensor kinases that share 62.5% sequence identity (*110*). Both of these proteins have a sensor domain, an ATPase domain and a kinase domain. As mentioned previously, the Dos regulon is induced by a range of related signals, including hypoxia, NO and carbon monoxide. All of these stimuli can be

recognized by DosS and DosT through the two GAF domains found within the sensor domain. The N-terminal GAF domain is designated the GAF A domain while the downstream GAF domain is designated the GAF B domain. These domains are so named because tandem GAF domains were first identified in cGMP phosphodiesterases, adenylate cyclases and FhlA from *E. coli* (*111*). These domains have been identified in a wide variety of organisms and are involved in signaling changes in response to O_2 and light stimulated pathways (*111*). The GAF A domain in DosS can bind a heme prosthetic group by its His149 residue. This histidine residue is also conserved in DosT, which has also been demonstrated to bind heme (*110*). The GAF A domains in DosS and DosT are the only known examples of GAF domains that associate with heme groups (*112*). The GAF A domain also requires Mg^{2+} as a cofactor for proper function (*113*).

1.5.6 DosS and DosT Induction Signals

While structurally similar, the induction signals for DosS and DosT differ. DosT was determined to bind O_2 directly through its heme group (*114*). The O_2-bound form of DosT is inactive, while a decrease in oxygen availability triggers its auto-catalytic activity (*110*). NO and CO lead to kinase activation by competitively inhibiting O_2 binding (*110*). The heme group has a much higher affinity for NO and CO than O_2 which is due in part to the GAF B domain (*115*).

In contrast, DosS can not bind O_2 directly. Rather, signaling is controlled by the oxidation state of the iron ion in the heme group. The ferric ion (Fe^{3+}) inhibits signaling, while the ferrous ion (Fe^{2+}) triggers DosS auto-phosphorylation (*116*). Therefore, the reduced form of DosS leads to signaling, while the oxidized form inhibits signaling. It

appears that the different substrate specificity between DosS and DosT is due to a glutamic acid at position 87 in DosS which blocks a channel in the GAF domain preventing O_2 from accessing the iron ion (*117*). Currently, the partners involved in the reduction of DosS remain unknown. Honaker et al. have shown that the size and reduction state of the menaquinone pool affects DosS signaling (*118*). The menaquinone pool plays a critical step in the electron transport chain (ETC), acting as intermediates in the transfer of electrons. As well, chemical inhibition of the ETC inhibits signaling through DosS (*118*). Thus it appears that DosS measures hypoxia using the reduction state of the ETC as a proxy (*118*). Reduced menaquinones do not reduce DosS *in vitro,* therefore, another intermediate molecule or cofactor is probably needed to induce DosS signaling (*119*). The major indicators of the redox (reduction-oxidation) state of a cell, NADH and NADPH, do not reduce DosS either. It appears that flavin nucleotides can directly reduce DosS *in vitro*, although the *in vivo* relevance of this observation is currently unknown (*119*).

In both DosS and DosT, signaling through the GAF A domain leads to a conformational change in the GAF B domain, which activates the kinase domain and leads to autophosphorylation of DosS at His395 and autophosphorylation of DosT at His392 (*107, 115, 120*).

1.5.7 The Mechanism of DosR Activity

DosR is a 217 amino acid protein composed of two domains, a receiver domain and a DNA binding domain. Its C-terminal DNA binding domain is a member of the NarL subfamily of DNA binding domains and its N-terminal activation domain belongs to the

CheY family of regulatory domains (*121*). The activation domain has 6 conserved residues involved in signal transduction; Asp8, Asp9, Asp54, Thr82, Tyr101 and Lys104 (*93*). Asp54 is phosphorylated by DosS or DosT, Thr82 can then associate with the phosphoryl group. A rearrangement of Thr82 causes Tyr101 to be repositioned into the hydrophobic core of the protein, causing a conformational change (*93*). This conformational change allows DosR to dimerize. Two DosR dimers can then dimerize again forming a tetramer of DosR (*93*). This tetramer is the transcriptionally active form of DosR. It can bind to DNA at conserved binding sites in the promoter region of Dos regulon genes. These binding sites are called DosR boxes and are found upstream of the majority of Dos regulon genes. Their consensus sequence is a variation of the palindromic sequence motif 5'-TTSGGGACTWWAGTCCCSAA-3' (S = C/G; W = A/T) (*122*). There are usually two or more DosR boxes in the promoter region of Dos regulon genes. Only phosphorylated DosR can associate with DNA (*123*). It has been suggested that a single DosR dimer will associate with the distal DosR box and can recruit another DosR dimer to the proximal box. The proximal box often overlaps with the -35 binding site element of SigA, the general sigma factor of *M. tb*. This may lead to SigA-dependent transcription of DosR genes (*124*).

Another level of complexity in DosR two-component signaling is that at least one other protein can modify the activity of DosR. Recently, Chao et al. have demonstrated that the serine-threonine kinase pknH can phosphorylate DosR on residues 198 and 205, leading to increased DosR signaling (*105*). This activation appears to happen independently of sensor kinase activation. Both PknH and DosS have been shown to cooperatively increase binding of DosR to DosR boxes and are both required for full

induction of the Dos regulon (*105*).

1.5.8 The DosR Promoter Region

The promoter region and regulation of *dosR* is very complex. As mentioned previously, *dosR* is part of a three gene operon, the genomic order is; *rv3134c-dosR-dosS*. There are six putative transcription start sites (TSS) upstream of *dosR* (*124, 125*). Some of these TSS are upstream of the whole operon while others are in the coding region of *rv3134c* and only lead to transcription of *dosR* and *dosS* (Figure 9). Transcription at these sites can either be constitutive or can be induced by different stimuli, e.g. hypoxia or nutrient starvation. The hypoxic induction of *dosR* is due to the presence of DosR boxes upstream of the operon. The major hypoxic TSS in the *dosR* operon is the T_H TSS (*124*). This causes a positive feedback loop, which leads to strong and rapid induction of *dosR* (*125*).

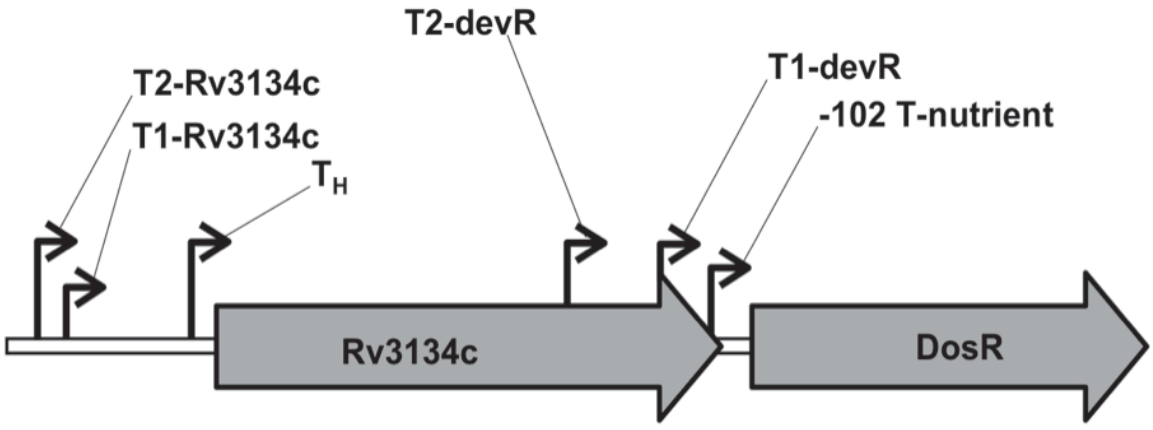

Figure 9: Diagram of the Promoter Region of the DosR operon
This diagram depicts the various transcription start sites (TSSs) in the promoter region of the DosR operon. Arrows represent TSS. The names of the TSSs come from the papers in which they were discovered (124, 125). Transcription at these TSS are induced by different stimuli and are active at different times.

1.5.9 The Role of DosR in Animal Models

The *in vivo* effects of ablation of DosR signaling remain ambiguous. The most straightforward way to determine the effect of a gene, e.g. DosR, is to ablate, or knock out (KO), the coding gene thereby eliminating functional protein from being produced. A study by Parish et al. demonstrated that mice infected intravenously with *M. tb* with ablated DosR died quicker and had higher organ bacterial burdens than mice infected with wild-type *M. tb* (*126*). On the contrary, Rustad et al. did not show any difference in organ bacterial burdens between a DosR KO strain of *M. tb* and a wild-type strain after aerosol infection (*38*). This was true for three different strains of mice, including the strain used in the study by Parish et al. Additionally, Malhotra et al. examined the organ bacterial burdens of guinea pigs after subcutaneous infections. They showed that *M. tb* with ablated DosR had lower bacterial burdens than wild-type *M. tb* (*127*). Finally, a series of experiments by Converse et al. demonstrated that *M. tb* with DosR KO showed a decrease in replication in mice and guinea pigs after aerosol infection, but no difference in replication after aerosol infection of rabbits (*128*). Therefore, the exact role of DosR expression in bacterial survival and pathogenesis is not yet understood and requires more study.

1.5.10 DosR Activity in the Beijing Lineage

The focus of our laboratory is to determine lineage-specific phenotypes of *M. tb* that can be associated with differences in pathogenesis. Among the phenotypes observed specifically in Beijing strains, one of special interest is the disregulation of Dos regulon

expression. While expression of the Dos regulon is normally induced by hypoxia and NO, Beijing strains constitutively overexpress the Dos regulon under aerobic conditions in liquid cultures with no stimuli present (*73*). Consequently, Beijing strains also constitutively overexpress DosR as it is a member of the Dos regulon. Constitutive overexpression of DosR and the Dos regulon is only found in modern Beijing strains and is not found in ancestral Beijing strains (Figure 10). The constitutive overexpression of DosR has also been validated by many other labs (*129, 130*). In modern Beijing strains the constitutive expression of DosR is on average 12-fold greater than ancestral Beijing strains. This difference in expression disappears after treatment with NO, an inducer of DosR signaling (*131*). As expression of the Dos regulon is associated with the adaptation of *M. tb* to the host, modulation of this pathway is a good candidate for a strain-specific difference that causes differences in pathogenesis.

1.5.11 DosT Mutation in Beijing Strains

Our group has also determined that modern Beijing strains have a deletion of a guanine residue at position 775 in the coding region of DosT. This causes a frameshift mutation and creates a putative stop codon 36 base pairs (bp) downstream (*131*). This mutation is found in the GAF B domain and is expected to lead to the truncation of DosT, causing translation of only the GAF A domain and part of the GAF B domain. All strains that constitutively overexpress DosR also have the DosT frameshift mutation (*131*). Although there is complete correlation between the presence of the DosT frameshift mutation and constitutive overexpression of DosR, The DosT mutation is not responsible for this phenotype. Overexpression of either the intact or truncated DosT in both modern

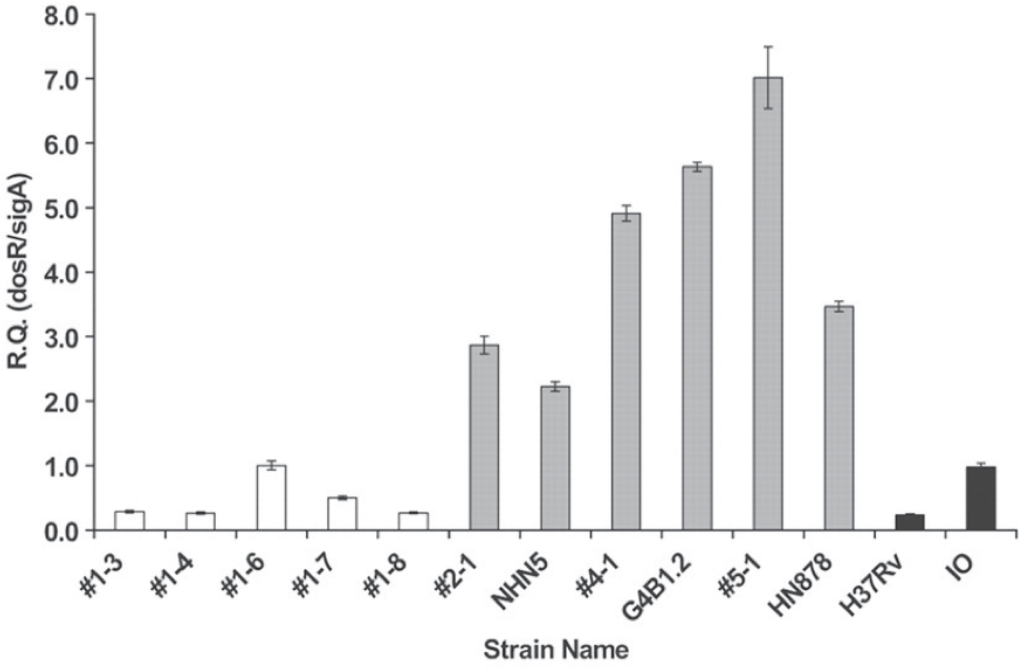

Figure 10: Constitutive Overexpression of *dosR* in Modern Beijing Strains

qRT-PCR analysis of *dosR* transcription in different lineages of *M. tb*. Expression levels of *dosR* in *M. tb* under liquid growth conditions were normalized to the sigA housekeeping gene (R.Q.= quantity of *DosR* relative to *sigA*). Error bars represent standard deviations. White bars represent ancestral Beijing strains, Grey bars represent modern Beijing strains and Black bars represent non-Beijing strains. For each sample, two independent samples were analyzed in triplicate. From: Fallow, A. et al,. *Strains of the East Asian (W/Beijing) Lineage of Mycobacterium tuberculosis Are DosS/DosT-DosR Two-Component Regulatory System Natural Mutants*. J. Bacteriol., 2010. **192**(8): p. 2228-2238, with permission.

Beijing and ancestral Beijing strains does not significantly impact expression of DosR or the Dos regulon (*131*). There are three hypothesized possibilities for the concomitant presence of the DosT mutation and the overexpression phenotype. (1) A mutation occurred causing DosR signaling to became constitutively activated and the DosT mutation occurred afterward in order to limit the amount of DosR signaling. (2) DosT is not required in modern Beijing strains so the mutation occurred without consequence (3). The DosT mutation could have occurred first. The constitutive signaling though DosR

could have been selected for afterward to facilitate DosR signaling without functional DosT present.

All three of these possibilities indicate that there is another cause for the constitutive overexpression of DosR and the Dos regulon besides the DosT mutation. This means that there are two possibilities for the phenotype found in modern Beijing strains. (1) There may be constitutive presence of induction signals or inhibition of inhibitory signals for either DosR or DosS. (2) There may be a novel partner in the DosR two-component system that is differentially modulated in modern Beijing strains.

1.5.12 The Implications of Constitutive DosR Signaling

There are some interesting implications pertaining to the overexpression of DosR in modern Beijing strains. As mentioned previously, Beijing strains appear to exhibit a number of phenotypes that make them more virulent. One of these is better intracellular fitness and survival. During infection *M. tb* is phagocytosed by host macrophages. The macrophage then produces NO in the phagolysosome. In non-Beijing strains of *M. tb*, the bacterium senses this release of NO and induces the Dos regulon. Some of these members are heat shock proteins that help the bacteria survive stress conditions. There is a lag phase between exposure to NO and response because these bacteria need to sense the stimuli, transcribe the RNA and translate sufficient protein to fortify the membrane. During this time period the NO radicals can damage the mycobacterial membrane and reduce cell viability. In modern Beijing strains the Dos regulon is constitutively induced, so its members are constitutively present in the bacteria. This means that modern Beijing strains would not experience the vulnerable lag period during initial phagocytosis and

may be less susceptible to NO oxidization. This hypothesis is currently under investigation in our laboratory. If proven correct, this may confer a survival advantage to modern Beijing strains and may explain in part the increased virulence observed in the Beijing lineage.

CHAPTER 2: RATIONALE & OBJECTIVES

Given that the Dos regulon is constitutively overexpressed in modern Beijing strains of *M. tb*, we attempted to determine the cause of this overexpression phenotype. We hypothesize that the difference in Dos regulon induction in modern Beijing strains (compared to ancestral Beijing and non-Beijing strains) is due to differences in regulation and/or function of the DosR two-component system. Furthermore, we hypothesize that differences in DosR two-component system signaling are the result of genetic differences unique to modern Beijing strains. We therefore set out to examine the entire genome for genes that modulate Dos regulon expression. To identify the genes responsible for the constitutive overexpression of the Dos regulon in modern Beijing strains, my project had the following four objectives:

1) To determine if modern Beijing strains display differences in known induction stimuli for the DosR two-component system.

2) To develop a reporter system capable of differentiating *M. tb* strains based on DosR two-component system signaling

3) To screen the entire genome of *M. tb* using transposon mutagenesis to discover novel genes affecting DosR reporter activity.

4) To identify how these genes affect reporter activity and how they impact Dos regulon induction.

By identifying genes that modify or interact with DosR, we hope to gain important information regarding the evolution of the unique pathogenic properties currently associated with the Beijing lineage.

CHAPTER 3: MATERIALS & METHODS

Unless otherwise specified, chemicals are from Sigma-Aldrich.

3.1 Media and Culture Conditions

All experiments using live *M. tb* were performed in a level three biosafety research facility in accordance with the standard operating procedures. Under standard growth conditions, *M. tb* isolates were grown in Middlebrook 7H9 broth (Difco) supplemented with 0.2% v/v glycerol, 0.05% v/v Tween-80 and 10% v/v albumin dextrose complex (ADC; 5% w/v bovine serum albumin fraction V, 2% w/v D-glucose and 0.81% w/v sodium chloride; NaCl). Liquid cultures were incubated at 37°C with rotation (2.0 rpm) in polystyrene culture bottles (Corning) at volumes less than one-fifth the total volume of the container. For growth on solid medium, *M. tb* was grown on Middlebrook 7H11 agar (Difco) containing 10% v/v oleic acid albumin dextrose complex (OADC; ADC with 0.6 ml/L oleic acid and 3.6 mM sodium hydroxide; NaOH). When necessary, media were supplemented with 50 μg/ml hygromycin and/or 25 μg/ml kanamycin. For cloning experiments, *Escherichia coli* was grown in Luria-Bertani media (Difco) or on LB-Agar plates (Difco) and antibiotics were added when necessary as follows: 200 μg/ml hygromycin and 50 μg/ml kanamycin. A list of all strains used in this study is presented in Table 1.

Table 1: *M. tb* Strains used in this Study

Strains	Identifying RD	Lineage	Group
H37Rv	pks15/1	Euro-American	non-Beijing
1-3 (95_1884)	RD 105	Group 1 Beijing	ancestral Beijing
HN878	RD 150	Group 4 Beijing	modern Beijing
B1.2 (G4B1.2)	RD 150	Group 4 Beijing	modern Beijing

RD:Region of difference

3.2 NO Quantification Assay

The NO quantification assay was performed on 50ml *M. tb* cultures collected after 24 h, 48 h and 72 h from an OD_{600}~0.2 starter culture using the Nitrate/Nitrite Colorimetric assay kit (Cayman Chemical Company). NO is very reactive and is rapidly converted to nitrate and nitrite. Thus, NO can be estimated by quantifying nitrate and nitrite levels. The procedure followed was identical to the manufacturers recommended protocol outlined in the manual. Significance was calculated using a two-tailed, unpaired T test.

3.3 Nucleotide Cycling Assay

For each replicate, two 15 ml cultures of *M. tb* at an OD_{600}~0.2 were collected. The cells were pelleted by centrifugation at 3,500 rpm for 15 min. The supernatant was removed and the cell pellet was resuspended in 100 µl 0.2 M HCl or 100 µl 0.2 M NaOH, for NAD(P)H and NAD(P) quantification respectively. The cells were then heated at 80°C for 20 min. Samples were then neutralized with 100 µl 0.1 M NaOH or 100 µl 0.1 M HCl, for NAD(P)H and NAD(P) respectively. Samples were flash frozen with dry ice.

For each replicate, 90 µl of both acid and base extractions were added to separate wells in a 96 well plate. For a standard, we used a 1:2 dilution series of NADH or NADPH ranging between 4 µM to 0.06 µM. 100 µl of cycling cocktail was added to each well and incubated for 3 min using a plate reader with automated dispenser (Wallac 1420, PerkinElmer). The cycling cocktail used for the NADH/NAD assay was composed of 2 ml 1 M bicine pH 8.0, 2 ml 100% ethanol, 2 ml 40 mM EDTA (pH 8.0), 2 ml 4.2 mM MTT (3-(4,5-Dimethylthiazol-2-yl)-2,5-diphenyltetrazolium bromide) and 4 ml 16.6 mM PES (phenazine ethosulfate). The cycling cocktail used for the NADPH/NADP assay was composed of 2 ml 1 M bicine pH 8.0, 2 ml 6.67 mM Glucose-6-phosphate, 2 ml 40 mM EDTA (pH 8.0), 2 ml 4.2 mM MTT and 4 ml 16.6 mM PES. For the NADH/NAD assay 10 µl of alcohol dehydrogenase solution (500 U/ml in 0.1 M bicine, pH 8.0) was dispensed and for the NADPH/NADP assay 10 µl of glucose-6-phosphate dehydrogenase solution (40 U/ml in 0.1 M bicine, pH 8.0) was dispensed. OD_{550} readings were taken every minute for 10 min. The concentration of NADH, NAD, NADPH and NADP were determined by comparing rate of change of OD_{540} compared to the standard curve. Significance was calculated using a two-tailed, unpaired T test.

3.4 Supernatant Exchange Assay

The supernatant exchange assay was performed on 50 ml cultures collected at an OD_{600} between 0.15-0.2. The cells were collected by centrifugation at 3,500 rpm for 15 min. Supernatants were removed and filter sterilized using a 0.2 µm syringe filter (Fisher). Filtered supernatant was then returned to the cell pellet of either the same or different lineage, dependent on the experimental conditions. Cultures were then incubated

for 6 h at 37°C with rolling. Samples were then processed according to the RNA extraction protocol outlined below. Significance was calculated using a two-tailed, unpaired T test.

3.5 RNA Extraction

RNA was isolated from early-log-phase *M. tb* cultures grown to an OD_{600} between 0.15-0.2. Cell pellets were collected by centrifugation at 3,500 rpm for 15 min. The supernatant was removed and the cell pellets were re-suspended in 1 ml TRIzol reagent (Invitrogen) and transferred to a 1.5 ml screw-cap tube containing 0.2 ml glass beads with a diameter of 0.1 mm (Biospec Products). Cells were disrupted in a homogenizer (Bio101/Savant, Fastprep FP120) by 3 pulses of 30 s that were each followed by a 3 min incubation on ice. The glass beads and cell debris were separated from the supernatant by a 2 min centrifugation at 12,000 rpm. The supernatant was then added to a new tube containing 200 µl of chloroform-isoamyl alcohol (24:1 [vol/vol]) and phase-separation was achieved by vigorous shaking followed by a 15 min centrifugation at 13,000 rpm. The upper aqueous phase was added to 500 µl isopropanol to precipitate the RNA and refrigerated for 16 h. RNA pellets were collected by a 15 min centrifugation, the isopropanol was removed, and the RNA pellet was washed with 70% ethanol. The 70% ethanol was removed and the pellet was air-dried at room temperature for 10 min. The RNA pellet was then dissolved in RNase-free water and incubated at 50°C for 10 min. 1 U/µl RNaseOUT (Invitrogen) was added and RNA was further dissolved by a 30 min incubation at 4°C. To remove contaminating DNA, The sample underwent a TURBO DNase (Ambion) treatment (2 U). Samples were then purified using an RNeasy minikit

(Qiagen). Afterwards the sample underwent another two TURBO DNase treatments (4 U). The reaction was stopped with the TURBO DNase inactivation reagent. The concentration of RNA in each sample was determined by spectrophotometry (OD_{260}, UVmini-1240, Shimadzu) and RNA was stored at -70°C. The absence of contaminating DNA was verified by qRT-PCR amplification of RNA samples.

3.6 1st Strand cDNA Synthesis

cDNA synthesis reactions each contained 300 ng of RNA, 1 µl random hexamer primers (250 ng/µl), 1 µl 10 mM dNTPs and dH_2O to 13 µl. Reactions were incubated at 65°C for 5 min followed by 1 min on ice. To this reaction mixture, a master mix containing the following was added: 1X SuperScript buffer, 5 mM DTT, 40 U RNase Out and 200 U of SuperScript III (Invitrogen). The cycling conditions were as follows: 25°C for 5 min, 55°C for 1 h and 70°C for 15 min. The cDNA was diluted 1:200 prior to use in qRT-PCR reactions.

3.7 qRT-PCR

For quantitative real-time polymerase chain reaction (qRT-PCR), primer sets were designed using Primer Express version 3.0 software (Applied Biosystems) and are listed in Table 1. qRT-PCR reactions were carried out using the Applied Biosystems 7300 Real-Time PCR System. Reactions were carried out in 20 µl volumes with 10 µl iTaq SYBR green supermix (Biorad), 300 nM of each primer and 4 µl diluted cDNA. Samples were assayed in triplicate in 96-well plates (Applied Biosystems). Cycling conditions were as follows: 2 min at 50°C, 10 min at 95°C and then 40 cycles of 15 s at 95°C and 1

min at 60°C. For each reaction, the amount of amplicon examined was normalized to the levels of the housekeeping gene *sigA*. A full list of all primers used in this study is presented in Table 2. For each set of qRT-PCR reactions, standard curves were prepared for relative quantification of both target and housekeeping (*sigA*) genes. To prepare these standard curves, a sample of *M. tb* genomic DNA of known concentration (2600 pg/µl) was diluted by 4-fold serial dilutions between 520 pg and 2.03 pg. The cycle threshold (cycle number at which fluorescence passed a set threshold) was plotted against the log of the input amount of standard DNA to generate a standard curve. Based on the standard curve, the SDS software (Applied Biosystems) calculated the mean quantity of target transcript. The relative quantity of gene expression was then determined by normalizing the mean quantity of the target transcript to the mean quantity of the *sigA* housekeeping gene. Significance was calculated using a two-tailed, unpaired T test. Standard deviation for each relative quantity was determined by the following formula where s is standard deviation and X is the mean quantity: $s = \sqrt{[(s_{target}/X_{target})^2 + (s_{sigA}/X_{sigA})^2]} \times (X_{target}/X_{sigA})$

3.8 Reporter Construction

The cloning strategies employed to construct the XylE reporter construct are as follows. A fusion polymerase chain reaction (PCR) was used to combine the reporter gene in frame with the DosR promoter. All PCR amplification for cloning purposes used the platinum *Pfx* polymerase (Invitrogen). PCR was carried out in 50 µl reactions that included 10–100 ng template DNA, 1 µM each of a forward and reverse primer (Invitrogen), 200 µM of deoxynucleotide triphosphates (dNTPs; Fermentas), 1.5 mM magnesium chloride (MgCl2; Fermentas), 1X *Taq* buffer with potassium chloride (KCl;

Table 2: List of Primers

Name	Sequence (5' to 3')	Function
DosR-RT-2-f	CTGGGCGATGGTTGTGGAC	qRT-PCR upstream of T_H TSS
DosR-RT-2-r	CTATCTCCCAGGGGCGTTG	qRT-PCR upstream of T_H TSS
DosR-RT-3-f	AACCGACGGGATGTATCCG	qRT-PCR downstream of T_H TSS
DosR-RT-3-r	CTCGGTTCACCGCCTCATC	qRT-PCR downstream of T_H TSS
DosR-RT-6-f	CTGCGCTGTCTGATCCTCAC	qRT-PCR amplification of *dosR*
DosR-RT-6-r	CAGCGCCCACATCTTTGAC	qRT-PCR amplification of *dosR*
HspX-f	GAATTCGCGTACGGTTCCTTC	qRT-PCR amplification of *hspX*
HspX-r	TGTCGTCCTCGTCAGCACC	qRT-PCR amplification of *hspX*
XylE-RT-1f	AGCAAGGCCCTGGAACACTA	qRT-PCR amplification of *xylE*
XylE-RT-1r	GCGTAGCACCAGGGAAAACTT	qRT-PCR amplification of *xylE*
katG-RT-2f	CGCCAAGGCCTGGTACAA	qRT-PCR amplification of *katG*
katG-RT-2r	TCGAAACTAGCTGTGAGACAGTCAA	qRT-PCR amplification of *katG*
MycoMar2f	GACCGAGATAGGGTTGAGTGTTG	Identification of transposon insertion
Mycomar1r	CCTTCTATCGCCTTCTTGACGAG	Identification of transposon insertion
XylE-seq-f	GCCTTTGAGTGAGCTGATACC	Sequencing XylE casette
XylE-seq-r	TGATGCCTGGCAGTCGATCG	Sequencing XylE casette
Kan-probe-f	GATGGATTGCACGCAGGTTCTC	Southern blot of transposon insertion
Kan-probe-r	CATGGGTCACGACGAGATCCTC	Southern blot of transposon insertion
xylE-f1	TGGGATCCGTTGCGTCTGTCATCGGTC	Cloning XylE reporter construct
xylE-r1	TACACCTTTGTTCATGCCGTCTCCTTCGCTGGG	Cloning XylE reporter construct
xylE-f2	AGCGAAGGAGACGGCATGAACAAAGGTGTAATGC	Cloning XylE reporter construct
xylE-r2	GCGGATCCTCAGGTCAGCACGGTCATG	Cloning XylE reporter construct

TSS: Transcription Start Site

Fermentas) and 1.25 U *Taq* polymerase (Fermentas). Where necessary, reactions were optimized with the addition of 5 or 10% dimethyl sulfoxide. The Bio-Rad i-Cycler thermocycling machine was used with the following conditions: a denaturation step was carried out at 94°C for 2 min, followed by 35 cycles of denaturation at 94°C for 10 s, annealing at 56°C for 10 s, and elongation at 68°C for 30 s. PCR products were electrophoresed on 1% agarose gels including ethidium bromide (EtBr) and visualized under UV light. The xylE-f1 and xylE-r1 primers were used to amplify the 132 bp upstream of the start codon of Rv3134c from *M. tb* genomic DNA. The xylE-f1 primer has an upstream *Bam*HI site and the xylE-r1 has a downstream 15 bp overlap with the

xylE coding sequence. The xylE-F2 and xylE-R2 primers were used to amplify the coding sequence of *xylE* from *Pseudomonas putida* (ATCC #33015) genomic DNA. The xylE-f2 primer has an upstream 19 bp overlap with the Rv3134c promoter and the xylE-r2 primer has a downstream *Bam*HI site. These two amplicons were isolated on a 1% agarose gel and purified by gel extraction using a QIAquik kit (Qiagen) as per the manufacturer's recommendations. A PCR reaction using both amplicons and the xylE-1f and xylE-2r primers was performed to create the reporter cassette. The site-specific integrative pMV306:hyg plasmid (*132*), was purified from transformed *E. coli* grown in LB broth with hygromycin using the Qiagen midi kit. The isolated reporter cassette as well as the pMV306:hyg vector were digested with *Bam*HI (Fermentas) at 37°C for 2 h. The vector was treated with calf intestinal phosphatase (Promega) for the removal of 5' phosphate groups at 37°C for 1 h. DNA was purified using MinElute Reaction clean-up kit (QIAgen) as per the manufacturer's recommendations. The ligation of the insert and the vector was carried out overnight at 16°C in a 20 µl reaction with 1X T4 ligase buffer, 5 Weiss U of T4 ligase (Fermentas), 1 µg insert and 0.1 µg vector. The resultant ligation mixture was dialyzed on a 0.025 µm pore cellulose membrane (Millipore) for 10 min to remove salt and used to transform electrocompetent *E. coli* cells (New England BioLabs 10-β competent *E. coli,* K12 strain). The electroporator (genePulser Xcell, Biorad) was set to 2.5 kV, 200 Ω and 25 µF and time constants in the range of 4.9-5.1 ms were achieved. Cells were incubated with SOC media (New England Biolabs) at 37°C for 1 h and then plated on LB with hygromycin. Single colonies were isolated into 3 ml of LB broth containing hygromycin. Plasmids were isolated with the Qiagen midi kit and the presence of the insert was confirmed by restriction digestion with *Bam*HI (Fermentas)

and by sequencing. All sequencing reactions were carried out at the *McGill* University and Génome Québec Innovation Centre

3.9 Transformation of Reporter Construct into *M. tb*

Cells from a 50 ml log-phase culture at an OD_{600} of 0.5-1.0 were collected by centrifugation at 3500 rpm for 15 min. Cells were first re-suspended in 50 ml of 10% glycerol, centrifuged, and then re-suspended in 25 ml of 10% glycerol, centrifuged again and then finally re-suspended in 500 µl of 10% glycerol. 250 µl of electrocompetent cells were incubated with the reporter plasmid DNA (1-2 µg) at 37°C for 10 min. The electroporator (BTX, Genetronics Inc.) was set to 2.5 kV, 1000 Ω and 25 µF and time constants in the range of 17–22 ms were achieved. Cells were incubated with 7H9 as recovery medium overnight at 37°C and then plated on 7H11 with hygromycin in 10-fold serial dilutions. Single colonies were isolated into 1 ml of 7H9 with hygromycin and after 3-weeks an aliquot was heated for 30 min at 85°C and then analyzed for the presence of the integrated reporter construct by PCR using the xylE-1f and xylE-2r primers.

3.10 Phage Transduction and Candidate Screening

30 ml cultures of a *M. tb* strain containing the reporter construct were grown up to late-log phase (OD_{600}~1.0). Cultures were divided into three 10ml aliquots, two for transduction and one for a no phage control (NPC). Cells were collected by centrifugation at 3,500 rpm for 15 min, washed once in 10 ml PAB buffer (7H9 without Tween-80) and resuspendend in 1 ml PAB. 1 ml of resuspended bacteria was added to 1 ml of high titer

ΦMycoMarT7 phagemid (10^{10} plaque forming units (pfu) /ml)(Multiplicity of infection = 10) (*133*). 1 ml of PAB was added to the NPC instead of phage. Samples were incubated at 37°C for 6 h to allow for phage adsorption, then added to 20 ml 7H9 and incubated for another 18-24 h at 37°C in a rolling incubator to allow for phage transduction and transposon integration. Cells were then collected by centrifugation at 3,500 rpm for 15 min, resuspended in 7.5 ml 7H9, aliquoted and stored in 25% glycerol at -70°C. One aliquot of transduced culture and NPC were thawed and 200 µl of 10^{0}-10^{-2} dilutions were plated on 7H11 with hygromycin and kanamycin. The plates from transduced cultures were used to titer cfu (colony forming units) in the glycerol stocks and the NPC was used to determine occurrence of spontaneous drug-resistant mutants.

Large-scale transductant screening was performed on plates with ~100-200 cfu/plate. When the majority of colonies had a diameter of ~2mm, colonies were sprayed with a catechol solution (100 mM Catechol, 50 mM K_2HPO_4, pH 7.5) using a glass CO_2-driven spray bottle (Supelco). Plates were sprayed entirely two times, with a 30 s break in between. Colour was allowed to develop between 3-5 min. Plates were examined for colonies displaying a difference in colour production. Candidate colonies were then picked using a sterile inoculating loop and used to start a liquid culture and re-streaked on 7H11 to verify that the picked colony was not a mixed culture. Liquid cultures were used to prepare glycerol stocks and DNA was extracted to determine the integration site of the transposon.

3.11 DNA Extraction

To isolate *M. tb* genomic DNA, liquid cultures were grown to an OD_{600} of 0.5 and then incubated 24 h with 0.2 M glycine to weaken the cell wall. Cell pellets were collected by centrifugation and re-suspended in an extraction buffer containing 25% w/v sucrose, 50 mM EDTA and 50 mM Tris, pH 8.0. Cells were then incubated 24 h with 500 µg/ml lysozyme for cell lysis. Next, an equal volume of proteinase K buffer (100 mM Tris, pH 8.0 and 1% SDS) with 400 µg/ml proteinase K was added to the cells and incubated at 55°C for 2 h. The sample was incubated at 70°C for 5 min and followed by an incubation on ice for 5 min. To eliminate contaminating RNA, 100 µg/ml RNase (Fermentas) was added to the sample and kept at 37°C for 30 min. DNA was purified by phase-separation with the addition of an equal volume of phenol-chloroform followed by vigorous mixing. The upper aqueous layer containing the DNA was transferred to a new tube and an additional chloroform extraction was performed. To precipitate the DNA, 40 µl of 3 M sodium acetate was added followed by 300 µl of isopropanol. The sample was incubated at -20°C overnight and the following day, the DNA pellet was collected by centrifugation and the supernatant was removed. The DNA pellet was washed with 70% ethanol and dissolved in TE buffer (10 mM Tris, 1 mM EDTA, pH 8.0) and stored at 4°C.

3.12 Determination of Phage Integration Sites

DNA was isolated from candidates by the protocol outlined above. 5 µg of DNA was digested using *Bam*HI (Fermentas) in a 60 µl reaction. Since the phagmid does not

have a *BamHI* site, this allows for the excision of the phagmid flanked on either end by genomic DNA. This digested DNA was then purified using a phenol:chloroform extraction. Briefly, the volume of the digestion reaction was brought up to 100 µl with TE buffer. 100 µl of Phenol:Chloroform:Isoamyl alcohol (25:24:1 [vol/vol/vol]) was added and mixed for 45 s. Reactions were centrifuged at 1,300 rpm for 15 min. The upper aqueous phase was removed and added to 100 µl Chloroform:Isoamyl alcohol (24:1 [vol/vol]) and mixed for 45 s. Reactions were centrifuged at 1,300 rpm for 15 min. The upper aqueous phase was then added to 250 µl 100% ethanol and 10 µl 3M sodium acetate. After incubation at -20°C for 30 min, tubes were spun at 1,300 rpm for 15 min. Supernatant was removed and pellet washed in 200 µl 70% ethanol. Pellets were air-dried and dissolved in 8.5 µl water. Digested DNA was heated at 65°C for 5 min and then placed on ice for 5 min. To each reaction, 0.5 µl T4 DNA ligase (Invitrogen) and 1 µl of ligase buffer were added. The reaction was incubated for 16 h at 16°C. The ligation reaction was used to transform pir+ *E. coli* (epicentre) by the protocol outlined above. DNA from transformants was isolated and sequenced using the Mycomar2F and Mycomar1R primers in order to determine the insertion site. Sequence data was analyzed by searching against the Tuberculist (Institut Pasteur) *M. tb* H37Rv sequence database using BLAST (Basic local alignment search tool).

3.13 Direct Extraction of RNA from Colonies on Solid Media

Liquid cultures of *M. tb* were grown to an OD_{600}~0.5. Cultures were diluted between 10^{-5}-10^{-7} and 200 µl were plated on 7H11 with hygromycin and kanamycin. Approximately 100 colonies were removed using a cell scraper (Sarstedt). Colonies were

transferred to a sterile petri dish lid and resuspended in 1 ml TRIzol (Invitrogen). The remainder of the procedure is identical to the RNA extraction protocol outlined above.

3.14 Catalase Assay

For each replicate, 50 ml of *M. tb* culture was collected at an OD_{600} between 0.45-0.55. The cultures were centrifuged at 3,500 rpm for 15 min. The supernatant was decanted and the cell pellet was washed twice with 5 ml $NaPO_4$ buffer (50 mM $NaPO_4$, pH 7.0). The cell pellet was resuspended in 500 µl of $NaPO_4$ buffer. The cells were transferred to a 1.5 ml screw-cap tube containing 0.2 ml glass beads with a diameter of 0.1 mm (Biospec Products). Cells were disrupted in a homogenizer (Bio101/Savant, Fastprep FP120) by 4 pulses of 45 s that were each followed by a 3 min incubation on ice. The tubes were spun at 13,000 rpm for 15 min. The supernatant was transferred to 0.2 µm spin columns (Milipore) and spun at 12,000 rpm for 2 min. The protein concentration of the lysate was quantified using the Biorad protein quantification kit according to the manufacturers specifications. Protein samples were diluted to ~400 µg/ml in $NaPO_4$ buffer and 200µl of diluted protein was transferred into a UV transparent cuvette (Sarstedt). 1 ml of H_2O_2 solution (10 mM H_20_2, 50 mM $NaPO_4$ buffer, pH 7.0) was added to the cuvette and the OD_{240} was measured every 30 s for 4 min. The ΔOD_{240}/time was used to calculate catalase activity by the formula:

Units/mg = $[\Delta OD_{240}/\text{min} \times 1000] \div [43.6 \times \text{mg enzyme/ml of reaction mixture}]$

Significance was calculated using a two-tailed, unpaired T test.

3.15 Reporter Inactivation Assay

For each replicate, 30 ml of *M. tb* culture was collected at an OD_{600} between 0.45-0.55. The cultures were then diluted to achieve similar cell counts. The cultures were centrifuged at 3,500 rpm for 15 min. Samples were then resuspended in 1ml $NaPO_4$ buffer (50 mM $NaPO_4$, pH 7.0). 100 mM H_2O_2 was added to cultures that underwent exogenous H_2O_2 treatment. Cultures were incubated at 25°C for 30 min and then transferred to 1.5 ml screw-cap tubes and centrifuged at 6,000 rpm for 10 min. The supernatant was discarded and the cell pellets were resuspended in 1 ml catechol solution (100 mM Catechol, 50mM K_2HPO_4, pH 7.5). Cultures were incubated at 25°C for 10 min and then transferred to 1.5 ml screw-top tubes containing 0.1 ml glass beads with a diameter of 0.1 mm (Biospec Products). Cells were disrupted in a homogenizer (Bio101/Savant, Fastprep FP120) by 3 pulses of 45 s that were each followed by a 3 min incubation on ice. Cells were spun at 13,000 rpm for 1 min and the supernatant was transferred to UV transparent cuvettes (Sarstedt). OD_{375} was read on a spectrophotometer (UVmini-1240, Shimadzu) and used to determine a quantitative measure of reporter activity. The sample with the lowest OD_{375} was subtracted from the remaining samples to set a baseline absorbance reading. Significance was calculated using a two-tailed, unpaired T test.

CHAPTER 4: RESULTS

4.1 Variation in DosR Two-Component System Stimuli Between Strains

In preliminary experiments aimed at discovering the underlying cause of the constitutive DosR regulon overexpression displayed by modern Beijing strains, we investigated the possibility that there existed differences in the presence/availability of DosR two-component system stimuli, i.e. NO or hypoxia, between modern Beijing strains and ancestral Beijing strains.

We began by determining if differences in DosR signaling between strains could potentially be accounted for by differences in endogenous NO production. We examined NO production by monitoring the formation of the NO-conversion products, nitrate and nitrite (NN), in the supernatant of a non-Beijing strain and a modern Beijing strain at 24 h, 48 h, and 72 h after setting up cultures in early log-phase (Figure 11A). Abundance of NN in the culture supernatant increased over time, nevertheless no significant variation in total NN production was observed between non-Beijing and Beijing strains at any time point. This result indicates that endogenous NO production does not account for the constitutive expression of the Dos regulon in modern Beijing strains.

As mentioned in the literature review, DosS does not directly monitor hypoxia. Rather, it responds to the oxidation state of menaquinones. The oxidation state of menaquinones is dependent on ETC signaling, which in turn is dependent on the redox balance of the bacilli. The latter is reflected in the relative levels of reduced and oxidized co-factors such as nicotinamide adenine dinucleotide (NAD or NADH) and nicotinamide

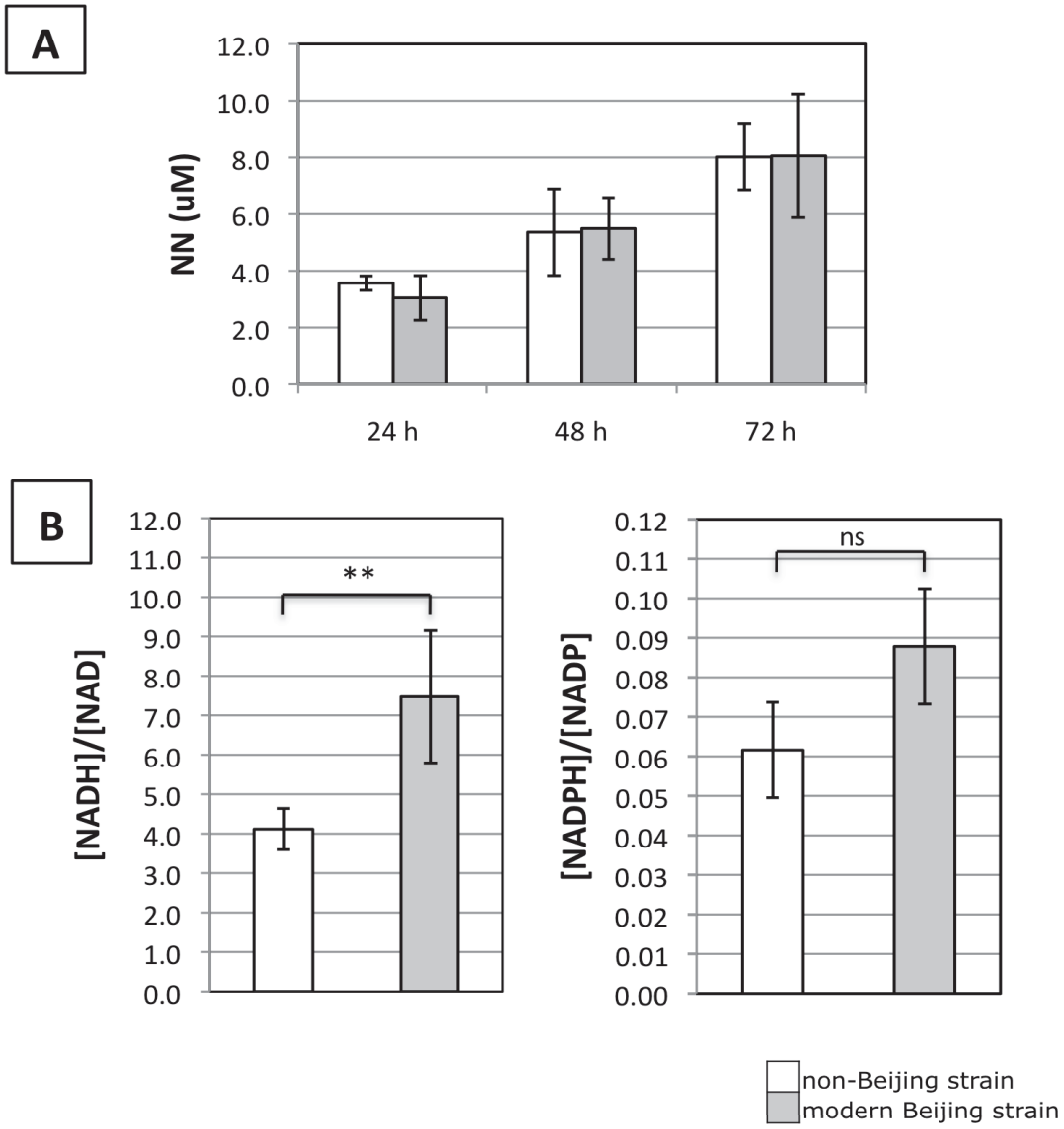

Figure 11: Variation in DosR Signaling Stimuli in Modern Beijing Strains
A) Quantification of endogenous nitric oxide (NO) production in different strains of *M. tb*. NO production can be estimated by quantifying Nitrate and Nitrite (NN) levels in the supernatant of bacterial cultures. We compared NN production between a non-Beijing strain (H37Rv) and a modern Beijing strain (B1.2). NN levels were quantified at 24h, 48h and 72h. Under all three timepoints there was no significant difference in NN levels between the non-Beijing and modern Beijing strains. Error bars represent standard deviation. Representative data from 3 biological replicates. **B)** Quantification of redox balance in different strains of *M. tb*. The NADH/NAD and NADPH/NADP ratios were compared between a non-Beijing strain (H37Rv) and a modern Beijing strain (B1.2) using a nucleotide cycling assay. The modern Beijing strain had a significantly higher NADH/NAD ratio compared to the non-Beijing strain. The modern Beijing strain also had a higher NADPH/NADP ratio, although this was not significant. Error bars represent standard deviation. Representative data from 3 biological replicates. **ns**: not significant, ** = $p<0.01$

adenine dinucleotide phosphate (NADP or NADPH). Therefore, we examined the role of hypoxia as a stimuli of the Dos regulon in *M. tb* by comparing the redox state of a non-Beijing strain and a modern Beijing strain using a nucleotide cycling assay, which measures the NADH/NAD ratio and NADPH/NADP ratio from bacterial lysates (Figure 11B). In these experiments, the modern Beijing strain showed a significantly higher NADH/NAD ratio, almost twice compared to the non-Beijing strain. The NADPH/NADP ratio was also elevated in modern Beijing strains (1.4 times higher), although not statistically significant. Thus, our preliminary results indicate that under standard *in vitro* culture conditions, the modern Beijing strains appear to exist in a more reductive metabolic state compared to non-Beijing strains, which could potentially account for the constitutive overexpression of DosR observed for the Beijing strains.

4.2 Cellular Localization of Factors Modulating Dos Regulon Expression

Next, to confirm whether any secreted factor could lead to the constitutive overexpression of the Dos regulon, we performed a supernatant exchange assay. We exchanged supernatants between modern Beijing and non-Beijing cultures for a period of 6 hours, and then analyzed transcription of the *dosR* gene and a Dos regulon gene (*hspX*) by qRT-PCR (Figure 12). 6 hours was chosen as previous studies had shown that *dosR* is induced rapidly in the presence of NO or under low oxygen conditions (*38*). We observed no difference in *dosR* or Dos regulon transcription levels between modern Beijing cultures incubated with modern Beijing supernatant or non-Beijing supernatant. We also observed no difference in *dosR* or Dos regulon transcription levels between non-Beijing cultures incubated with non-Beijing supernatant or modern Beijing supernatant. These

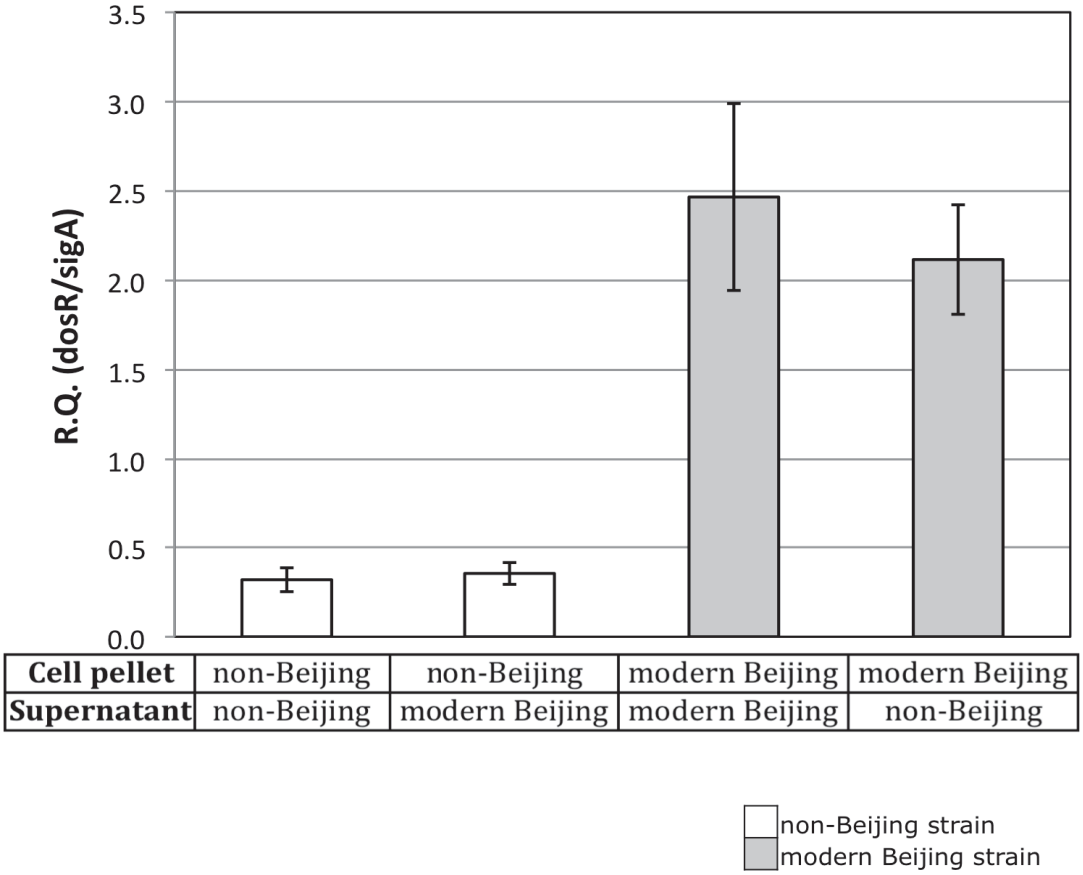

Figure 12: Identification of the Cellular Location of DosR Signaling Co-Regulators
The cellular localization of the factor leading to constitutive overexpression of DosR in modern Beijing strains was determined by qRT-PCR using a supernatant exchange assay. A non-Beijing strain (H37Rv) and a modern Beijing strain (B1.2) were grown in the presence of supernatant taken from both modern Beijing and non-Beijing cultures. The supernatant appeared to have no significant effect on *dosR* expression in both non-Beijing and modern Beijing strains as quantified by qRT-PCR. The relative quantity of *dosR* was normalized to the *sigA* housekeeping gene with the standard curve method of relative quantization. Error bars represent standard deviation. Representative data from 3 biological replicates.

results indicate that no factors responsible for constitutive DosR signaling are secreted but are rather intracellular or membrane-bound.

4.3 Development of a DosR-Dependent Reporter System

In order to further examine the cause of constitutive overexpression of DosR in modern Beijing strains and as a potential avenue to understand the basis for the altered redox balance that appears to exist within these strains, we performed a whole genome mutagenesis screen to identify novel partners that influence DosR signaling. In order to perform this screen, we first needed to develop a reporter system to easily differentiate strains based on their expression of *dosR*.

For our reporter system to be a monitor of Dos regulon induction, we needed to use a promoter region that was only transcribed in a DosR-dependent manner. Dos regulon promoter elements contain DosR box consensus sequences. The promoter region we selected included the 132 bp upstream of the start codon of Rv3134c. This region encompasses the T_H TSS, which contains two DosR boxes and has a mapped transcription start site 40 bp upstream of the start codon (*124*). To validate the dependence of this promoter region on DosR, we examined mRNA levels via qRT-PCR using oligonucleotide primers immediately upstream and downstream of the transcription start site (Figure 13A). We compared transcription surrounding this TSS in a non-Beijing strain and a modern Beijing strain as well as a non-Beijing DosR KO strain and a modern Beijing DosR KO strain. No amplification upstream of the TSS was detected for any strains, indicating that there are no other TSSs upstream that could affect transcription of the reporter gene. No transcription downstream of the TSS for the DosR KO in both

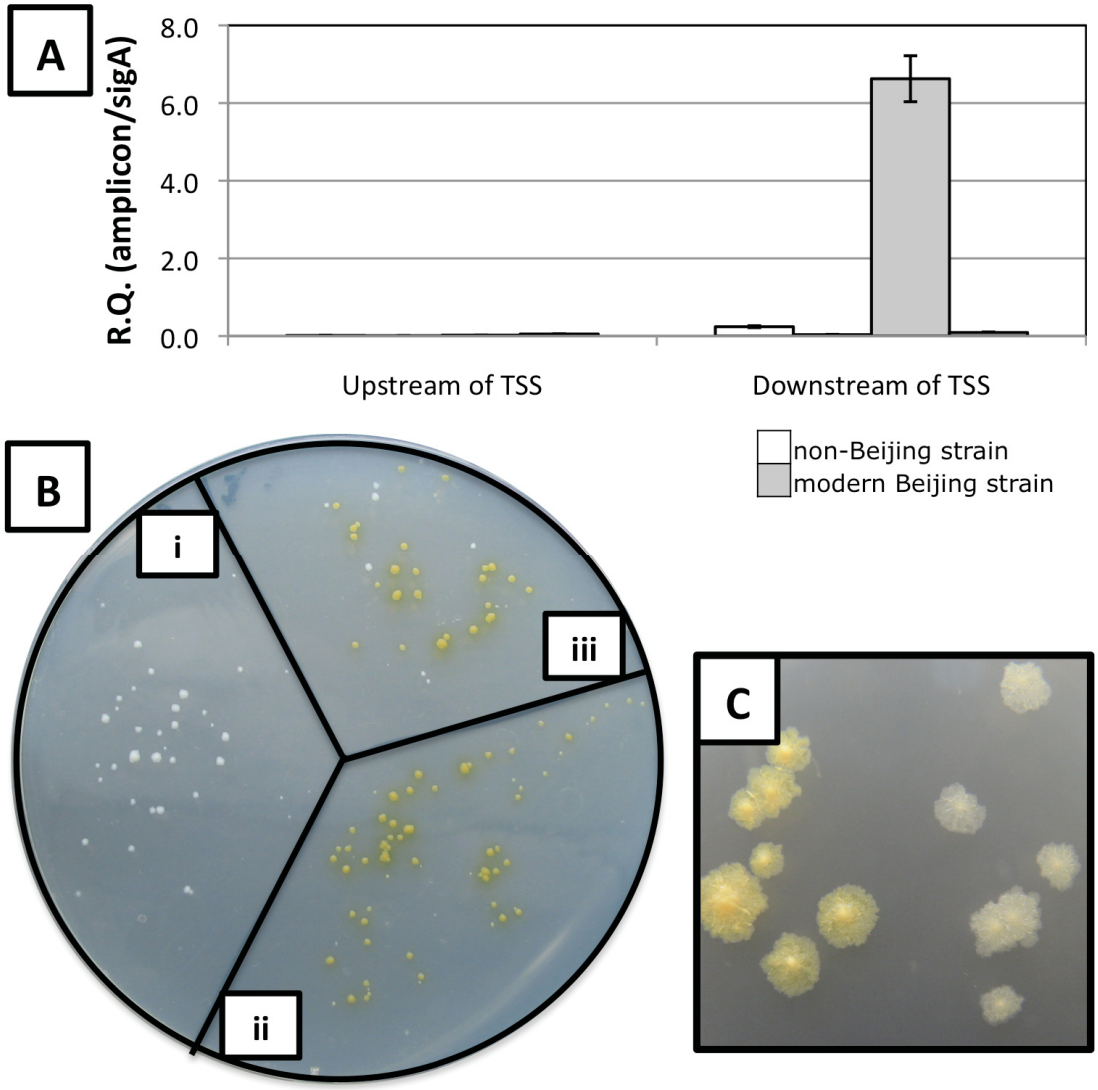

Figure 13: Reporter Construct Validation

A) Validation of the promoter region for the reporter construct. mRNA levels were quantified immediately upstream and downstream from the TSS of the T_H promoter using qRT-PCR. No transcription was identified upstream of the TSS for any condition. Similarly, no amplification was seen using primers located downstream of the TSS for both the non-Beijing (H37Rv) DosR KO strain and the modern Beijing DosR KO strain (B1.2). There was significantly more transcription in the modern Beijing strain compared to the non-Beijing strain. The relative quantity of promoter amplicon was normalized to the *sigA* housekeeping gene with the standard curve method of relative quantitation. Error bars represent standard deviation. Data from 3 technical replicates. **B)** Solid 7H11 media plate 5 min after catechol treatment. i) modern Beijing strain (B1.2) with empty vector. ii) modern Beijing strain with pdosRXylE. iii) Mixture of modern Beijing strain with either empty vector or pdosRXylE. Colonies with empty vector appear white after catechol treatment while colonies with reporter plasmid appear yellow. **C)** Solid media plate 5 min after catechol treatment. Modern Beijing strain (HN878) is on the left while an ancestral Beijing strain (1-3) is on the right. HN878 colonies are more yellow than 1-3 colonies after identical catechol treatment.

modern and non-Beijing strains was also shown in this analysis, suggesting that the TSS is entirely dependent on DosR for transcription induction. The modern Beijing strain has over 27-fold more transcription downstream of the TSS compared to the non-Beijing strain (Fig. 13A) and is consistent with the variation in *dosR* over-expression we observe between these strain types (*131*). Together these observations suggest that this promoter region is ideal for control of the reporter gene.

The reporter gene we used for our assay is the *xylE* gene, which codes for catechol-2,3-dioxygenase. This enzyme catalyzes the conversion of catechol into 2-hydroxymuconic semialdehyde, a yellow coloured product. As *M. tb* growth rates are very slow (24h doubling time), we performed our screen directly on colonies on solid media. This allowed us to screen many candidates simultaneously. In order to confirm that our reporter gene would allow us to screen colonies on solid media, we transformed a modern Beijing strain with either the *xylE* reporter construct (pdosRXylE) or empty vector and then plated these strains either individually or as a mixed culture. As is shown in figure 13B, we were able to visually differentiate between colonies with the empty vector (white) or reporter construct (yellow). We were also able to validate our visual differentiation by screening for the presence of the *xylE* cassette by PCR (results not shown).

We also verified that we could visually separate modern Beijing strains from ancestral Beijing and non-Beijing strains. We transformed a modern Beijing strain (HN878) and an ancestral Beijing strain (1-3) with the pdosRXylE construct. We plated the strains on the same plate (Figure 13C). After identical catechol treatment, the modern Beijing strain was significantly more yellow compared to the ancestral Beijing strain.

This confirms that our reporter system can differentiate between modern Beijing strains and ancestral Beijing strains. Furthermore, the correlation between DosR expression levels and reporter activity suggests that the difference in reporter activity is due to the intrinsic difference in DosR signaling between the two strains.

4.4 Transcriptional Analysis of *M. tb* Under Various Growth Conditions

Previous work in our lab had described the constitutive overexpression of DosR and members of the Dos regulon in modern Beijing strains under early log-phase liquid growth conditions (*131*). However, for our reporter screen, we wanted to screen candidates directly on solid media. Early aerobic liquid culture conditions are potentially very different to solid media growth conditions, so we wanted to examine expression of *dosR,* a Dos regulon gene (*hspX*) and our reporter gene (*xylE*) under a variety of growth conditions to verify that reporter system activity and specificity did not vary. We examined gene expression under three liquid growth conditions: early-logarithmic growth (OD_{600}~0.2), mid-logarithmic growth (OD_{600}~0.4) and stationary phase (OD_{600}>1.0). We examined expression in a modern Beijing strain, an ancestral Beijing strain and a non-Beijing strain. We also analyzed expression of the Dos operon and reporter in modern Beijing and non-Beijing DosR KO strains.

First we examined expression of *dosR* under these different growth conditions (Figure 14A). We were able to replicate the constitutive overexpression of *dosR* in modern Beijing strains under early-logarithmic growth. Modern Beijing strains express *dosR* approximately 7 fold higher than the non-Beijing or ancestral Beijing strains. This trend continues for both the mid-logarithmic growth phase as well as during the

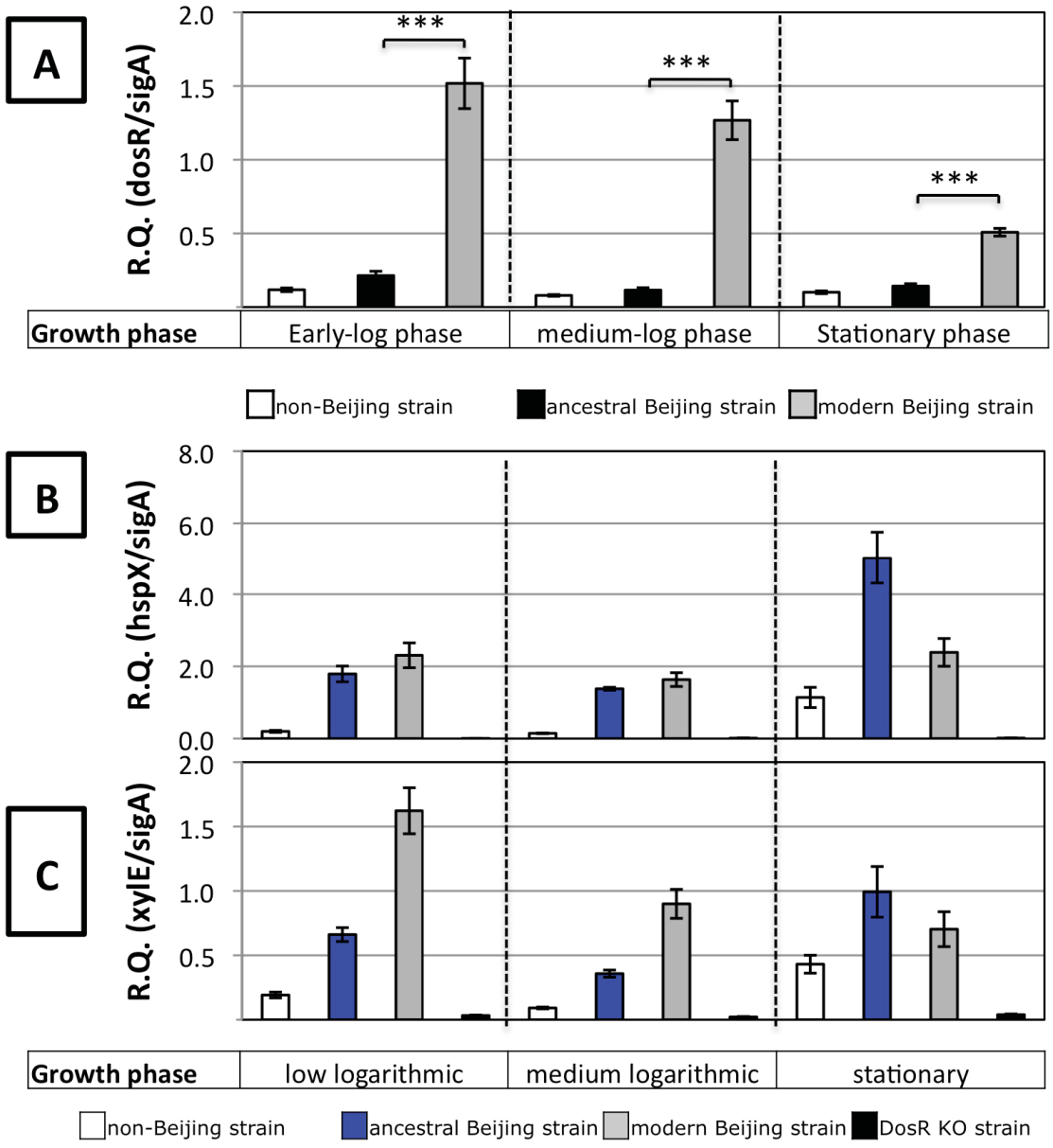

Figure 14: *M. tb* Gene Expression Under Different Liquid Growth Conditions
qRT-PCR analysis of gene expression in a non-Beijing strain (H37Rv), an ancestral Beijing strain (1-3), a modern Beijing strain (HN878) and a DosR KO modern Beijing strain (HN878). Samples analyzed under early-log growth phase, medium-log growth phase and stationary phase. **A)** *dosR* transcript levels. Under all growth conditions the modern Beijing strain expresses significantly more *dosR* than either the ancestral Beijing strain or the non-Beijing strain. **B)** *hspX* transcript levels. **C)** *xylE* expression levels. For both *hspX* and *xylE* we observed no expression under any growth condition for the DosR KO strains. In early and mid-logarithmic cultures, it appears that the ancestral Beijing strain expresses levels of *hspX* and *xylE* comparable to modern Beijing strains and significantly higher than non-Beijing strains. For stationary phase cultures, there is less of a distinction between non-Beijing and Beijing cultures. The relative quantity of transcript was normalized to the *sigA* housekeeping gene with the standard curve method of relative quantization. Error bars represent standard deviation. Representative data from 2 biological replicates. *** = $p<0.001$

stationary growth phase. These results show that there is a clear difference in *dosR* expression between ancestral and non-Beijing strains compared to modern Beijing strains under all liquid growth conditions.

We also investigated the effect of growth conditions on a member of the Dos regulon by analyzing the expression of *hspX*, one of best-studied and earliest identified members of this regulon (*134*). Likewise, we examined *xylE* expression to see how its expression correlated with genes in the Dos regulon. As shown in Figures 14B and 14C, the same expression trends were detected for both *hspX* and our reporter gene *xylE*. We observed no expression of *hspX* or *xylE* under any growth condition for the DosR KO strains. These results indicate that transcription of *hspX* and *xylE* are entirely dependent on DosR. Our data also show that there is an imperfect correlation between *dosR* expression and *hspX* or *xylE* expression. In low and mid-logarithmic cultures, it appears that the ancestral Beijing strain expresses levels of *hspX* and *xylE* comparable to modern Beijing strains and significantly higher than non-Beijing strains. This trend is less apparent for stationary phase cultures, where there is less of a distinction between non-Beijing and Beijing cultures. The difference in expression patterns between *dosR* and *hspX* suggest that although DosR is required for *hspX* expression, there are other partners within the bacteria that modulate expression of members of the Dos regulon. Importantly, this finding adds considerable weight in support of our hypothesis that modifiers of *dosR* expression/function exist and may play a role in the development of the constitutive DosR phenotype displayed by Beijing strains.

The correlation between *xylE* and *hspX* indicate that expression of the *xylE* reporter appears to be a good indicator for expression of the Dos regulon gene, *hspX*,

under the growth conditions analyzed. Together with the fact that expression of the reporter (*xylE*) is entirely dependent upon the expression of *dosR*, this finding validates the reporter system for use in the subsequent transposon mutagenesis screening.

4.5 Whole-Genome Mutagenesis Using Transposon Mutagenesis

We examined the potential role of all genes in *M. tb* on DosR signaling using transposon mutagenesis. Transposon mutagenesis allows for the insertion of a single copy of a transposable element randomly into the mycobacterial genome. This allows for the individual ablation of all genes in the mycobacterial genome. By performing transposon mutagenesis in a strain containing the pdosRXylE reporter plasmid, we can determine if ablation of any gene affects *dosR* expression and/or DosR regulon induction.

Transposon mutagenesis screening was performed within four different strain backgrounds, two modern Beijing strains (B1.2 and HN878), an ancestral Beijing strain (1-3) and a non-Beijing strain (H37Rv). These strains were used to perform two different types of screening. (1) A screen looking for a decrease in reporter expression within the two modern Beijing strains with high constitutive reporter expression. (2) A screen looking for increased reporter expression in an ancestral Beijing strain and a non-Beijing strain with low constitutive reporter expression. To achieve complete coverage of the genome we aimed to screen ~20,000 colonies for each of the four strain backgrounds.

In total we screened 78,934 candidates (Table 3). The number of screened candidates allowed us to get a theoretical coverage rate of one insertion approximately every 110 bp in the mycobacterial genome for each of the two screens. For the screen

Table 3: Transposon Screening List

Strain	Constitutive DosR expression	Transductants	Positives
B1.2	High	20,370	16
HN878	High	19,064	48
H37Rv	Low	18,440	17
1-3	Low	21,060	6
	Total:	78,934	87

monitoring loss of XylE activity in B1.2, a modern Beijing strain, we identified 16 candidates (Figure 15A) that appeared to have reduced reporter expression following catechol treatment. Of these candidates, 10 had an insertion within the coding region of the *xylE* reporter gene. The other modern Beijing strain, HN878, yielded 48 candidates for decreased reporter activity (Figure 15B). Of these candidates, 8 were determined to be caused by an insertion in XylE. The fact that we were able to identify colonies bearing insertions within the reporter itself was a further validation of the utility of our screening protocol.

For the gain of expression screen in H37Rv, the non-Beijing strain, we discovered 17 candidates with altered *xylE* activity (Figure 15C). Of these candidates, 7 were determined to have the transposon inserted upstream of the reporter gene. The ancestral Beijing strain, 1-3, which underwent transposon mutagenesis yielded 6 potential candidates. Of these, 2 were determined to be caused by an insertion upstream of the reporter (Figure 15D). In each case, insertion of the transposon sequence upstream of the reporter gene appeared to enhance *xylE* transcription as verified by qRT-PCR and again validates our screening protocol for identifying genes that enhance DosR function in wither the non-Beijing or ancestral Beijing strain backgrounds.

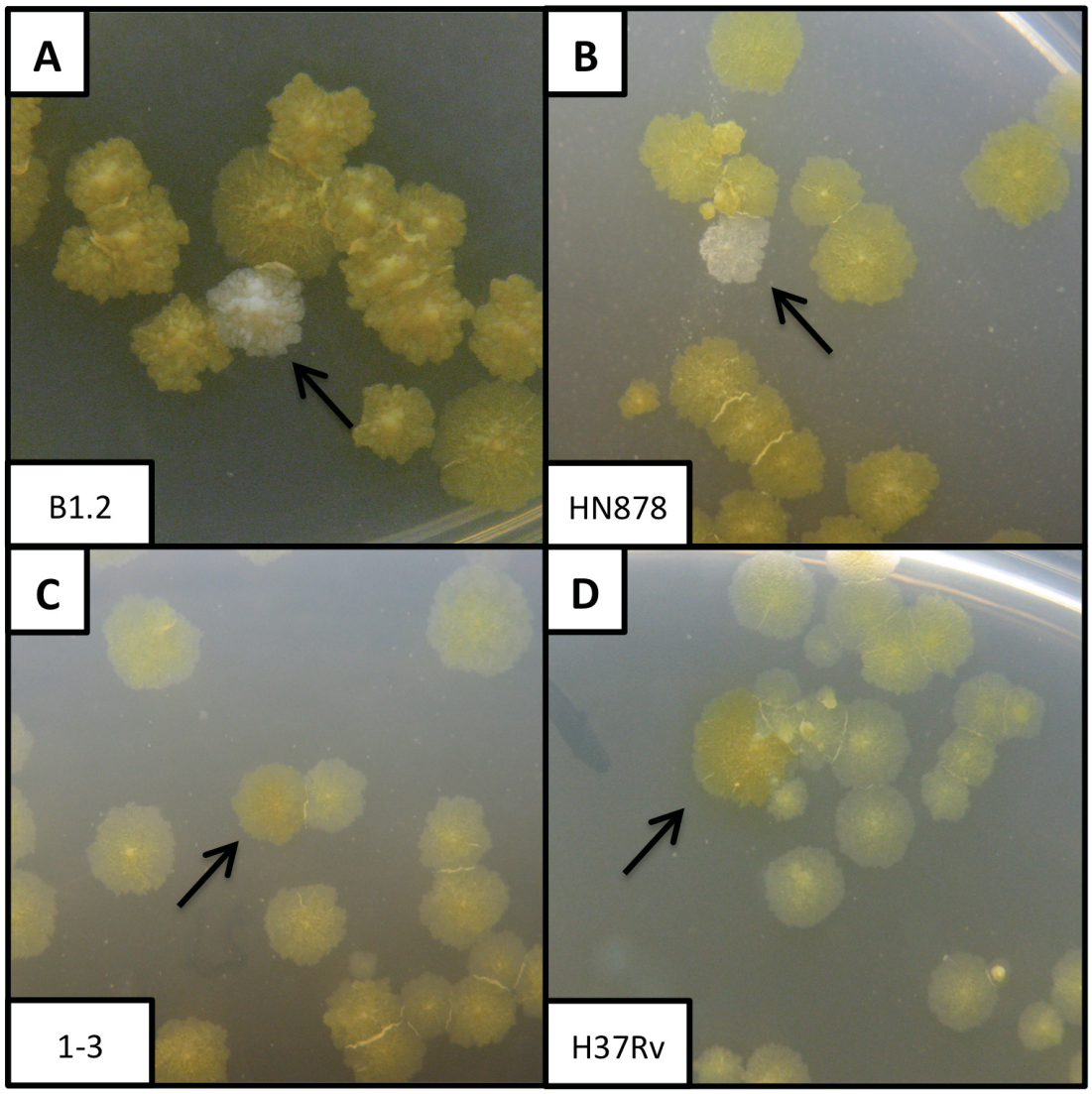

Figure 15: Screen for Reporter Modulation in *M. tb*
Example images of candidates identified by the transposon mutagenesis screen. The modern Beijing strains, B1.2 (**A)** and HN878 (**B**), have high constitutive expression of the reporter. We selected candidates with lower expression of the reporter. The ancestral Beijing strain (1-3 (**C**)) and the non-Beijing strain (H37Rv (**D**)) have low constitutive expression of the reporter. We selected candidates with higher expression of the reporter. Selected candidates are indicated by arrows.

In total this screen identified 60 transposon insertion events in *M. tb* coding regions. Of these, 6 genes had more than one independent insertion event in the same loci. Therefore, we have identified 49 loci in the genome of *M. tb* that appear to affect reporter expression (Table 4). We also cross-referenced all candidates against the TB Phylogeographic Diversity Sequencing Project database (*135*), to determine if any genes had SNPs unique to modern Beijing strains (Table 3) that could account for altered expression/function of the particular gene in question. Within our candidates we identified 4 non-synonomous mutations unique to the modern Beijing lineage.

4.6 Functional Analysis of Candidates Identified by Transposon Mutagenesis

The Pasteur Institute maintains a database, known as Tuberculist, of information on all genes in *M. tb* and sorts them into 10 separate functional classifications (*136*). For a preliminary analysis of our transposon mutants, we wanted to determine if any functional category was enriched within the set of genes identified in our transposon mutagenesis screen compared to the proportions normally found in the genome. To develop a baseline of functional classifications, we chose 100 non-essential genes at random (*50*). We then sorted these genes by their functional classifications (Figure 16A). As well, we sorted all the genes identified in our screen into the same functional classifications (Figure 16B). The two groups were then compared to see if genes in any specific classification were enriched compared to the baseline proportions found in *M. tb* (Figure 16C). There was very high agreement between the proportions found in our baseline group compared to the transposon mutants. The two classifications that demonstrated enrichment in transposon mutants were lipid metabolism, which increased

Table 3: Genes Identified by Transposon Mutagenesis

List of all loci identified in the transposon mutagenesis screen. The strain heading indicates the strain background in which the candidate was identified. The function of the gene comes from Tuberculist (Pasteur Institute) while the SNP data come from the Tuberculosis database. SNP can refer to either a nucleotide deletion or a non-synonymous point mutation. Genes highlighted in the same color represent multiple insertions within the same locus.

Strain	Locus	Name	Function	SNP
H37Rv	Rv1319c	Rv1319c	possible adenylate-cyclase	None
H37Rv	Rv1750c	fadD1	fatty-acid-CoA ligase	None
H37Rv	Rv2294	Rv2294	Probable aminotransferase	None
H37Rv	Rv2339	mmpL9	possibly fatty acid transport	219C del
H37Rv	Rv2374c	hrcA	heat inducible transcriptional repressor	None
H37Rv	Rv2425c	Rv2425c	conserved hypothetical protein	None
H37Rv	Rv2485c	lipQ	carboxylesterase	R60L SNP
H37Rv	Rv3296	lhr	ATP-dependent helicase	None
H37Rv	Rv3440c	Rv3440c	hypothetical protein	None
H37Rv	Rv3484	cpsA	hypothetical protein	None
B1.2	Rv0023	Rv0023	possible transcriptional regulatory protein	None
B1.2	Rv0337c	AspC	aspartate aminotransferase	None
B1.2	Rv0410c	pknG	ser/thr protein kinase	None
B1.2	Rv2298	Rv2298	conserved hypothetical	None
B1.2	Rv2917	Rv2917	conserved membrane protein	None
B1.2	Rv3668c	Rv3668c	protese	None
1-3	Rv0245	Rv0245	oxidoreductase	None
1-3	Rv2931	ppsA	type-I polyketide synthase	L1194R SNP
1-3	Rv2935	ppsE	type-I polyketide synthase	None
1-3	Rv2940c	mas	multifunctional mycocerosic acid synthase	None
HN878	Rv0032	bioF2	8-amino-7-oxononanoate synthase	None
HN878	Rv0050	ponA1	bifunctional penicillin-binding protein	None
HN878	Rv0122	rv0122	hypothetical protein	None
HN878	Rv0498	rv0498	conserved hypothetical protein	None
HN878	Rv0770	Rv0770	dehydrogenase/reductase	None
HN878	Rv0950c	Rv0950c	conserved hypothetical protein	None
HN878	Rv0964c	Rv0964c	hypothetical protein	None
HN878	Rv1206	fadD6	fatty-acid-CoA ligase	None
HN878	Rv1206	fadD6	fatty-acid-CoA ligase	None
HN878	Rv1299	prfA	peptide chain release factor 1	None
HN878	Rv1436	gap	glyceraldehyde 3-phosphate dehydrogenase	None

Table 3: Genes Identified by Transposon Mutagenesis (Continued)

Strain	Locus	Name	Function	SNP
HN878	Rv1617	pykA	pyruvate kinase	None
HN878	Rv1617	pykA	pyruvate kinase	None
HN878	Rv1811	MgtC	Mg2+ transport ATPase	None
HN878	Rv1819c	Rv1819c	ABC transporter	None
HN878	Rv1821	secA2	preprotein translocase ATPase	None
HN878	Rv1908c	katG	catalase-peroxidase-peroxynitritase	None
HN878	Rv1908c	katG	catalase-peroxidase-peroxynitritase	None
HN878	Rv1908c	katG	catalase-peroxidase-peroxynitritase	None
HN878	Rv1908c	katG	catalase-peroxidase-peroxynitritase	None
HN878	Rv1909c	furA	catalase-peroxidase-peroxynitritase	None
HN878	Rv1909c	furA	ferric uptake regulation protein	None
HN878	Rv1910c	Rv1910c	hypothetical exported protein	None
HN878	Rv2024c	Rv2024c	hypothetical protein	None
HN878	Rv2024c	Rv2024c	hypothetical protein	None
HN878	Rv2048c	pks12	Probable polyketide synthase	None
HN878	Rv2112c	Rv2112c	putative proteasome component	None
HN878	Rv2123	PPE37	PPE family protein	507c del
HN878	Rv2241	aceE	pyruvate dehydrogenase E1 component	None
HN878	Rv2395	Rv2395	conserved membrane protein	None
HN878	Rv2445c	ndkA	nucleoside diphosphate kinase	None
HN878	Rv2513	Rv2513	hypothetical protein	None
HN878	Rv2524c	fas	fatty-acid synthase	None
HN878	Rv2530c	Rv2530c	conserved hypothetical protein	None
HN878	rv2705c	rv2705c	conserved hypothetical protein	None
HN878	Rv2727c	miaA	isopentenylpyrophosphate transferase	None
HN878	Rv2727c	miaA	isopentenylpyrophosphate transferase	None
HN878	Rv3439c	Rv3439c	conserved alanine and proline rich protein	None
HN878	Rv3593	lpqF	hypothetical protein	None
HN878	Rv3777	Rv3777	related to quinone oxidoreductase	None

from 6.0% to 13.3% (7.3% enrichment) and intermediary metabolism and respiration, which increased from 17.0% to 26.7% (9.7% enrichment). This analysis indicated that a higher than expected proportion of genes identified in the transposon mutagenesis screen are involved in cellular metabolism and respiration. This suggests that genes involved in metabolism and respiration may be directly or indirectly affecting the activity of our DosR-dependent reporter. The latter finding was particularly interesting in light of our

earlier finding that the modern Beijing strains displayed an altered redox balance with respect to non-Beijing or ancestral Beijing strains.

To eliminate the possibility that candidates had multiple transposon insertions we probed the mycobacterial genome for the transposon by Southern Blotting (results not shown). In all the strains we have examined so far, there has only been a single transposition event in the genome of every candidate.

4.7 Transcriptional Analysis of Transposon Mutant Candidates

In order to validate our candidates we examined *xylE* and *dosR* expression in all of our transposon mutants. We initially attempted to validate this phenotype under the same conditions where constitutive overexpression of DosR is most apparent, liquid cultures grown to early-log phase (OD_{600}~0.2). We examined all 60 candidates that contained insertions by qRT-PCR (results not shown). Surprisingly, we did not observe a reproducible modulation of either *xylE, dosR,* or *hspX* expression for any of the candidates. For some candidates, we also re-examined expression of the preceding genes in mid-log (OD_{600}~0.5) and stationary phase (OD_{600}>1.0) cultures. For all conditions there was no reproducible modulation of the target genes. Thus, despite the careful validation of the reporter system that included demonstrating its dependence on DosR, our data indicate that none of the candidates identified through the transposon mutagenesis screen appear to have an alteration in *dosR* (or the *xylE* reporter) gene expression.

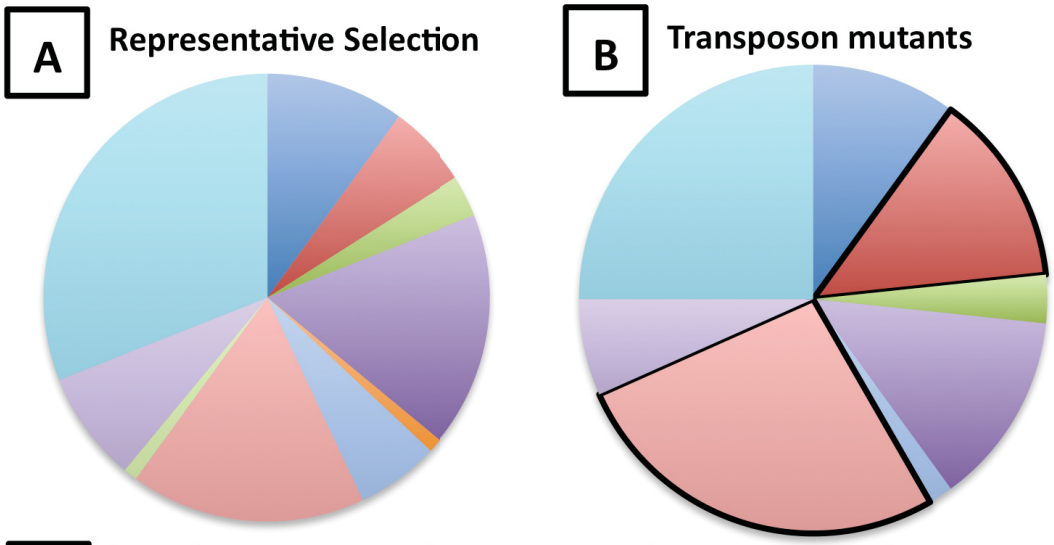

C

Code	Functional classification	representative selection (%)	transposon mutants (%)	Enrichment (%)
0	virulence, detoxification, adaptation	10.0	10.0	0.0
1	lipid metabolism	6.0	13.3	**7.3**
2	information pathways	3.0	3.3	0.3
3	cell wall and cell processes	17.0	13.3	-3.7
4	stable RNAs	0.0	0.0	0.0
5	insertion seqs and phages	1.0	0.0	-1.0
6	PE/PPE	6.0	1.7	-4.3
7	intermediary metabolism and respiration	17.0	26.7	**9.7**
8	unknown	1.0	0.0	-1.0
9	regulatory proteins	8.0	6.7	-1.3
10	conserved hypotheticals	31.0	25.0	-6.0

Figure 16: Functional Analysis of Candidates Identified by Transposon Mutagenesis
Analysis of transposon mutants by their functional classifications. **A**) Pie chart representing the functional annotation of 100 randomly selected, non-essential genes from *M. tb.* **B**) Pie chart representing the functional annotation of the 60 loci with transposon insertions. The pie chart sections are coloured according to the the code colours in the table below **C**) The enrichment column indicates the total proportion of the classification in transposon mutants minus the proportion in the representative selection. Functional classifications that show an enrichment in genes identified in the transposon screen are highlighted. The two classifications that shown an enrichment in transposon mutants are genes involved in lipid metabolism and genes involved in intermediary metabolism and respiration.

4.8 Transcriptional Analysis of Colonies on Solid Media

Since we could not demonstrate a quantitative difference in Dos regulon expression for our transposon candidates grown under aerobic liquid culture conditions, we decided to examine gene transcription levels from RNA directly extracted from colonies grown on a solid media. This was done to examine the possibility that the altered reporter phenotypes we observed for our candidate clones were specific to growth on solid agar-based media.

After developing a novel RNA extraction method for colonies on solid media (see Materials & Methods) the mRNA levels of several candidates were re-examined by qRT-PCR. The results again showed no difference in *xylE* transcript levels between candidates and the parental strains (results not shown). Unexpectedly, our quantification of *xylE* from RNA extracted directly from colonies failed to show any difference in transcript levels between modern Beijing and ancestral Beijing strains (Figure 17). Moreover, we were able to identify transcription of the reporter in strains with an ablated *dosR* locus. Together, these results show that when grown on solid 7H11 media, the reporter system is transcribed independent of DosR and is expressed at similar levels in modern Beijing and ancestral Beijing strains. Unfortunately, this indicates that the screen we performed was not specifically screening for alterations in Dos regulon expression, rather we appear to have been selecting genes that affect reporter activity in another manner.

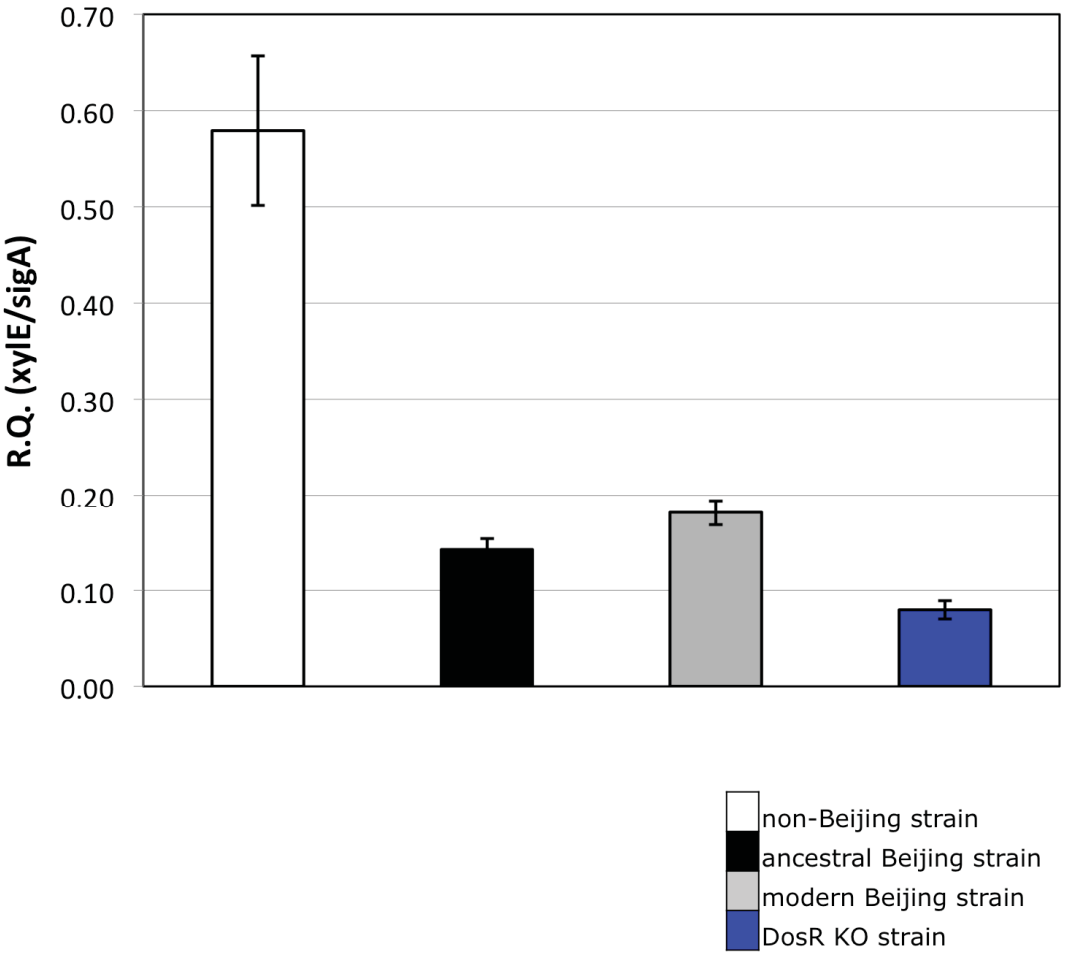

Figure 17: Transcriptional Analysis of Colonies on Solid Media
qRT-PCR analysis of RNA extracted directly from colonies on solid media. Results failed to show any difference in transcript levels between modern Beijing and ancestral Beijing strains. As well, there is transcription of the reporter in the DosR KO strain. There is also increased reporter expression in the non-Beijing strain compared to all other strains. The relative quantity of *xylE* was normalized to the *sigA* housekeeping gene with the standard curve method of relative quantization. Error bars represent standard deviation. Data from a single biological sample per strain background

4.9 Determination of the Role of KatG on Reporter Construct Activity

In the HN878 modern Beijing strain background we identified 7 candidates with a transposon insertion within a locus 2,129 bp in size. The probability of these insertions occurring by chance alone is $<1.5*10^{-8}$ %. This locus contains an operon containing *furA, katG and rv1907c* (Figure 18A). KatG is the major catalase enzyme in *M. tb*, FurA is a protein responsible for the regulation of KatG expression (*137*) and Rv1907c is a protein of unknown function. Catalases are responsible for degradation of H_20_2. Whilst searching for a potential explanation for our transposon screening data, we identified a publication demonstrating that H_20_2 can oxidize the active site of XylE, rendering it inactive (*138*). In order to determine if ablation of *katG* was directly affecting the activity of our reporter system, we performed a catalase assay to monitor catalase activity in transposon mutants and parental strains (Figure 18B). All transposon mutants with an insertion within the *katG* locus lacked endogenous catalase activity, which provides an explanation for why these particular clones were identified through our transposon mutagenesis assay. Interestingly, we also noticed a difference in the endogenous catalase activity in modern Beijing (strains B.1.2 and HN878) compared to other strains of *M. tb*. The fact that there is a higher level of catalase within these strains is consistent with the strong yellow coloration we observed for the modern Beijing reporter strains following catechol treatment. Conversely, the lower endogenous catalase levels in the non-Beijing and ancestral Beijing lineages coincides with their lack of coloration in the presence of catechol.

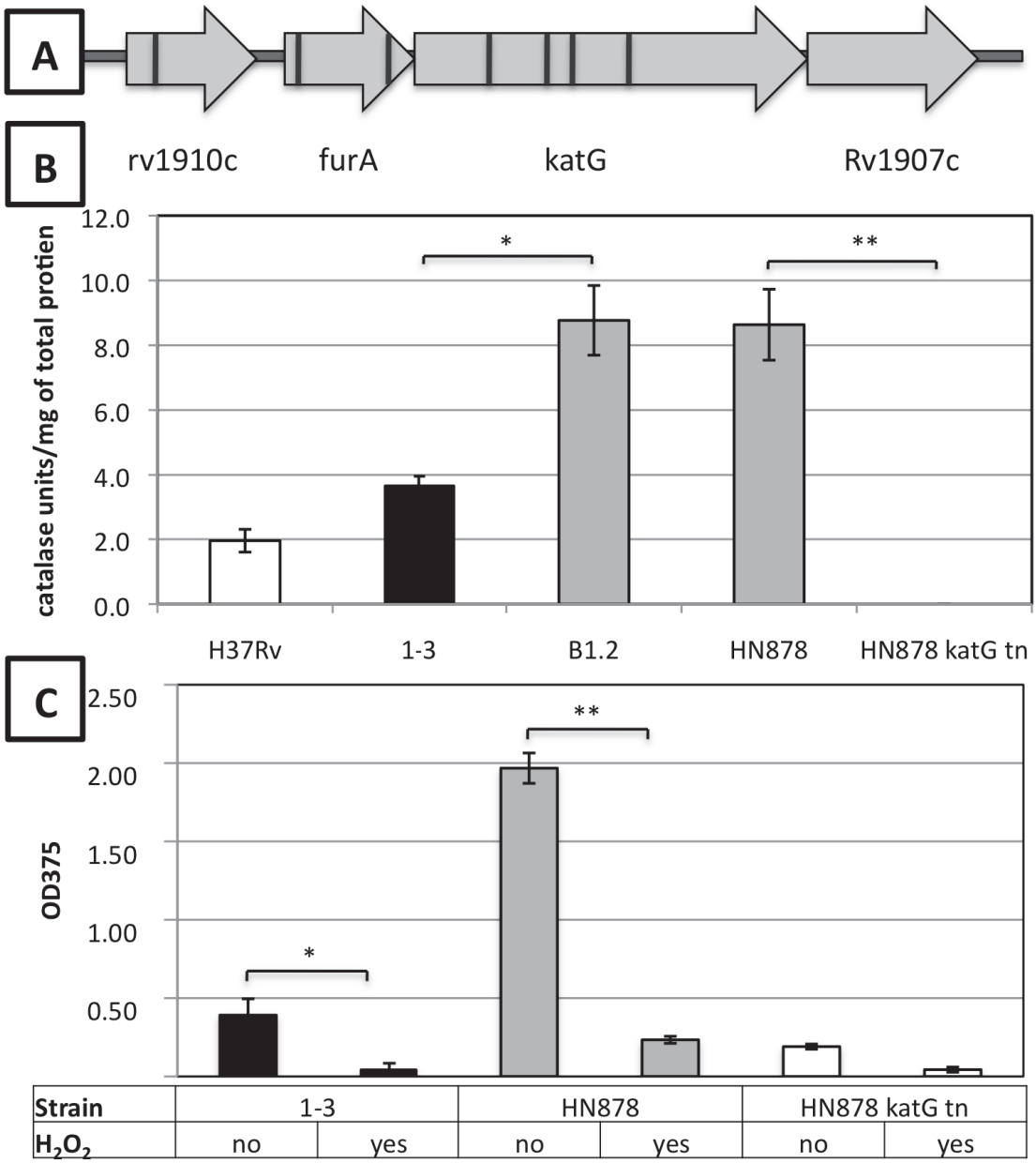

Figure 18: Effect of H_2O_2 on Reporter Activity

A) Schematic representing the operon coding for *katG*. The approximate location of independent transposon insertion sites are indicated by the black lines. **B**) Catalase activity of different strains of *M. tb*. The modern Beijing strains (B1.2 and HN878) had comparable catalase activity. There was no measurable catalase activity in the modern Beijing strain with ablated *katG* coding region (HN878 katG tn). Both the ancestral Beijing strain (1-3) and the non-Beijing strain (H37Rv) had significantly lower catalase activity than either modern Beijing strain. Error bars represent standard deviation. Representative data from 2 biological replicates **C)** Effect of exogenous H_2O_2 on reporter activity. $OD_{375\ i}$ is a measure of catechol conversion. HN878 has significantly more XylE activity than 1-3 or HN878 with ablated KatG (HN878 katG tn). Treatment with exogenous H_2O_2 decreases XylE activity for all strain backgrounds. Error bars represent standard deviation. Representative data from 2 biological replicates. *=$p<0.05$. **=$p<0.01$

Finally, we also tested the effect of exogenous H_2O_2 on the activity of the reporter (Figure 18C). We examined catechol conversion in an ancestral Beijing strain, a modern Beijing strain and a modern Beijing strain with an ablated *katG* locus. Without H_2O_2 treatment, the modern Beijing strain is more yellow than the ancestral Beijing strain (5 fold) and the strain with an ablated *katG* locus is completely white. After treatment with exogenous H_2O_2, both the modern Beijing and ancestral Beijing strains showed a significant decrease in reporter activity. Together, these results suggest that insertions in the *katG* locus do not cause differences in Dos regulon signaling, but rather they directly lead to the inactivation of the XylE reporter protein.

Research performed in our lab has previously demonstrated that DosR and members of the DosR regulon are constitutively overexpressed in modern Beijing strains. In this thesis, we have investigated the cause of this overexpression in order to gain a better understanding of the regulation of DosR two-component signaling in *M. tb* and to gain insight into the underlying phenotypic differences that distinguish Beijing from non-Beijing strains.

We began by examining if there was any variation in induction signals unique to modern Beijing strains. *M. tb* normally responds to exogenous NO produced by host macrophages during an infection by inducing the Dos regulon. However, for all modern Beijing strains, constitutive overexpression of DosR is observed in liquid cultures without NO present, so exogenous NO is not responsible. However, there is precedence for bacteria producing endogenous NO (*139*), therefore, we investigated if endogenous NO production accounts for constitutive DosR signaling. We did not observe any indication that there was any difference in endogenous NO production between any of the different strains of *M. tb* studied. Therefore we eliminated endogenous NO production as a potential cause for constitutive DosR signaling.

We also examined if hypoxia affected DosR signaling. As discussed previously, Beijing strains do not have a functional DosT, and DosS senses hypoxia by monitoring the reduction state of the ETC. We did observe higher ratios of NADH/NAD and NADPH/NADP in a modern Beijing strains compared to a non-Beijing strain. NADH is one of the substrates for the ETC, so a higher ratio of NADH/NAD could lead to a more

reductive ETC. Menaquinones are a major electron carrier in the ETC. A more reduced ETC would lead to a more reduced menaquinone pool, which has been demonstrated to lead to DosS signaling (*118*). This in turn could account for higher constitutive expression of the Dos regulon in Beijing strains. At present we do not understand what is causing this shift in the redox balance within the modern Beijing lineages, nor have we confirmed that this is directly responsible for the constitutive overexpression of DosR. The answers to these questions will form the focus of ongoing investigations in the laboratory.

The overexpression of the Dos regulon in Beijing strains must be due to the differential modulation of one or more cellular factors. They could either be protein factors or metabolic factors. To narrow down the identity of these factors, we wanted to determine if any of them are excreted or if they all remain cytoplasmic. The supernatant exchange assay we performed demonstrated that none of the factors responsible for constitutive overexpression of the Dos regulon are excreted factors. This eliminates some potential types of factors; small proteins or peptides involved in cell-to-cell communication, e.g. quorum sensing (*140*) and small excreted metabolic molecules that can cross the cell membrane, e.g. oxide radicals. Therefore, the factors that are differentially modulated in modern Beijing strains must remain in the cytosol or must be embedded in the membrane of *M. tb*.

To initiate a search for genes that could potentially impact DosR function and give rise to the constitutive Beijing phenotype, we next developed an *in vitro* screen based on the XylE reporter that was placed under the control of a DosR-dependent promoter region. To understand how our reporter system is regulated we need to look at

the results from section 4.4 and section 4.8 together. In section 4.4 we show that our reporter system is entirely dependent on DosR and differentially expressed between ancestral Beijing and modern Beijing strains under many different growth conditions. This is also correlated to a difference in reporter activity as observed for colonies on solid media (Figure 13C). Together these results suggested that our reporter was differentially transcribed in colonies on solid media. When our qRT-PCR validation of candidates failed to show any differences in transcription of DosR, we decided to look at transcriptional differences from RNA extracted directly from colonies on a plate. Although a rather unorthodox approach, since this is the same condition under which the colonies were initially screened it should provide the most accurate method of quantifying transcription under our screening conditions. Contrary to what we expected, this analysis failed to show any differences between ancestral or modern Beijing strains for *xylE* expression and also failed to show an ablation of reporter activity in the DosR KO strain. There is increased reporter expression in the non-Beijing strain but this is most likely an artifact due to its differential growth rate compared to the other strains. This demonstrates that our reporter system functions correctly under aerobic liquid conditions, but does not behave as a suitable DosR-dependent reporter during growth on solid media.

As discussed in the literature review, the promoter region for Rv3134c is very complex and transcription from many TSSs are induced by a wide variety of stimuli (Figure 9). Although we validated that there was no transcription occurring upstream of our TSS is liquid media (Figure 13A) there could be transcription induced upstream during growth on solid media. This must be due to differences in the environment between the two media. It may be due to the differences in growth time, differences in

oxygen exposure or nutritional differences. To overcome this problem in the future, we would need to either screen our candidates under aerobic liquid culture conditions or develop a new DosR dependent promoter for the reporter system. Screening candidates based on the XylE reporter in aerobic liquid culture is not feasible due to the extended growth times of *M. tb* and the lack of a simple quantitative liquid screening technique that is suitable for high-throughput screening. In the future, it may be feasible to generate additional reporter constructs based on luciferase or *lacZ* that allow us to screen a more limited number of clones in a liquid culture-based assay. If we were to change the promoter region, we would use an entirely artificial promoter region constructed with only two-DosR boxes and an overlapping SigA binding site. This artificial promoter would eliminate the possibility that other TSSs exist in the promoter region we selected.

Ultimately, even though our screen did not appear to detect genes involved in DosR signaling, it still appears to be screening for something affecting reporter activity. This is illustrated by the difference in colour of our candidate colonies (Figure 13C). As well, we have identified six loci with multiple proximal independent insertions (Table 3). The odds of getting these multiple insertions by chance are very low (between 0.1% and $1.5*10^{-8}$ % dependent on the size of the loci and number or insertion events). Therefore, it is likely that these loci are significant in terms of reporter expression/function and our ability to identify these loci did not occur by chance. Although not followed-up in the present study, we have also identified SNPs specific to modern Beijing strains that occur in or around the genes identified in the transposon mutagenesis screen (Table 3). A modern Beijing-specific SNP could account for the natural constitutive overexpression of the Dos regulon, therefore these loci warrant future research. There is another important

consideration for the loci we have identified in our transposon screen. As mentioned in the materials & methods section, the transposon contains T7 transcription sites driving transcription of genes proximal to the insertion site. Therefore, any phenotype we observed can be either due to the ablation of the gene in which it is inserted or due to increased transcription of downstream genes. This is why we have identified insertions upstream of our reporter gene in ancestral Beijing and non-Beijing strains that cause increased reporter activity.

Although it appears that our screen is not a good indicator for Dos regulon expression in colonies on solid media, we have demonstrated that modern Beijing strains and ancestral Beijing strains have differential reporter activity in colonies on solid media (Figure 13C). Since transcription of the reporter seems to be similar between strains when assayed through qRT-PCR (Figure 17), the most likely explanation is that there is a post-translational modulation of the activity of the reporter protein between strains. In this regard, we decided to determine the effect of the *katG* locus on reporter activity. We identified 7 candidates with a transposon insertion proximal to this gene, so we were confident this locus had an effect on reporter activity. KatG is the major catalase enzyme in *M. tb*. Catalases degrade H_2O_2 into water and oxygen. After completing our transposon screening assay, we identified a publication that demonstrated that H_2O_2 can inactivate XylE by oxidizing its active site (*138*). Therefore, we hypothesized that a strain with an ablated *katG* locus could not produce KatG and may not be able to degrade hydrogen peroxide. If strains produce endogenous H_2O_2 as a natural by-product of aerobic respiration, strains without KatG may produce levels of H_2O_2 sufficient to inactive the XylE reporter. We proved this by demonstrating that our transposon mutants with

insertions surrounding *katG* had no catalase activity (Figure 18B). We also demonstrated that our reporter system is inactivated by treatment with exogenous H_2O_2 (Figure 18C). Together, these findings can explain our observation of decreased reporter activity independent of DosR two-component system signaling.

Interestingly, we also identified an intrinsic difference in catalase activity between modern Beijing strains compared to ancestral and non-Beijing strains. Different strains of *M. tb* can have different levels of catalase activity (*141*), although this has never been examined within the Beijing lineage before. Increased catalase activity in modern Beiing strains could explain why we observed the difference in reporter activity (Figure 13C) without the concomitant difference in reporter gene expression on solid media (Figure 17). We did not detect a difference in *katG* expression in modern Beijing strains (results not shown), so differences in catalase activity must be due to regulation by another cellular factor. Ultimately, if we wanted to perform this screen again to determine DosR signaling coregulators, we would need to use another reporter protein whose activity is not affected by H_2O_2. For example, we could use the *lacZ* reporter gene from *E. coli*. *M. tb* is impermeable to many substrates for *lacZ* so we would use 4-Methylumbelliferyl beta-D-galactopyranoside (MUG) for our detection reagent. MUG is permeable to the membrane of *M. tb* and is modified by *lacZ* to produce a fluorescent compound that may yield more quantitative results than *xylE*.

The preliminary examination of functional classifications indicated that there was an enrichment in genes involved in metabolism in candidates identified in the transposon mutagenesis screen. This implicated metabolic pathways and the ETC in reporter activity. To further clarify what pathways were involved in reporter activity, we wanted to identify

if any of the genes from the transposon screen were members of similar pathways. If the genes were involved in similar pathways, it could implicate these pathways in reporter modulation. We identified a number of enzymes involved in glycolysis and other pathways involved in precursor formation for the TCA cycle in our loss of reporter expression screen in modern Beijing strains. We identified two insertions in *pykA*, the pyruvate kinase enzyme for *M. tb*. This is the terminal enzyme in glycolysis and produces pyruvate for the TCA cycle. We also identified an insertion in *aceE*, which codes for a subunit of the pyruvate dehydrogenase complex and an insertion in *gap*, the enzyme that codes for glyceraldehyde 3-phosphate dehydrogenase. All of these enzymes are required for metabolism through glycolysis. Our analysis also identified two insertions in *fadD6*. This enzyme in involved in the degradation of fatty acids into acetyl-CoA, which is another precursor for the TCA cycle. All of these insertions would inhibit the TCA cycle. The major purpose of the TCA cycle is to produce reducing equivalents (NADH and $FADH_2$) for induction of the proton motive force via the ETC. We also identified a potential partner of the electron transport chain, Rv3777, which is a putative quinone oxidoreductase. Although ablation of these genes does not appear to affect DosR signaling, they may be involved in modulating XylE activity. Endogenous H_2O_2 is a by-product of ETC signaling (*142*). Therefore, these transposon insertions could indirectly affect H_2O_2 production through the ETC, leading to differential XylE activity as was seen for the transposon insertions located within the *katG* locus.

Finally, although we were not able to determine the cause of constitutive overexpression of the Dos regulon in Beijing strains, we made an interesting discovery; that modern Beijing strains have higher catalase activity than ancestral Beijing and non-

Beijing strains. This could have *in vivo* relevance for survival of *M. tb* in the macrophage. Exogenous H_2O_2 is produced by macrophages to help destroy bacteria in a processes know as a respiratory burst (*141*). If modern Beijing strains have constitutively higher catalase activity, they may be better able to survive exogenous H_2O_2 produced by the host macrophage and may be better able to survive inside the macrophage compared to ancestral Beijing or non-Beijing strains. Indeed, several previous studies have noted enhanced replication rates of Beijing isolates within *in vitro* cultured human and mouse cell lines (*89*) and enhanced virulence within several animal models (*75*). Differential survival rates of modern vs. ancestral Beijing strains in macrophages is currently being investigated in our laboratory and the availability of the *katG* transposon mutants identified in the current study will aid greatly in understanding the potential role of catalase in enhancing the survival and virulence of the modern Beijing lineages.

CHAPTER 6: CLOSING REMARKS: SUMMARY & CONCLUSIONS

In this thesis we identified a number of new phenotypes that appear to be unique to modern Beijing strains of *M tb*. First, we demonstrated that at least a subset of modern Beijing strains have a more reductive redox environment. Second, we demonstrated that modern Beijing strains have higher endogenous catalase activity compared to ancestral Beijing strains. The implications of these novel findings await further investigation.

For the major part of this thesis we performed a large-scale mutagenesis screen of 78,934 colonies, identifying 60 candidates that affected our reporter expression. Although our thorough analysis of promoter activity demonstrated the strain-specific expression and DosR dependency of our reporter system in many different growth phases, it appears that under the conditions we ultimately used for our screen (colonies grown on solid agar plates), the reporter system is constitutively expressed in all strain backgrounds. Therefore, these candidates do not appear to be responsible for the constitutive overexpression of the Dos regulon in modern Beijing strains. We demonstrated that we were instead screening for genes that affected H_2O_2 levels within the bacteria or that affected XylE activity in some other way. This means that our candidates may still be relevant to understanding virulence mechanisms unique to the Beijing lineage of *M. tb*.

In summary, the results presented here show that there are significant physiological differences unique to modern Beijing strains of *M. tb* that could be implicated in the differences in virulence attributed to the Beijing lineage. The data presented in this thesis further reinforces the need for scientists and clinicians to understand strain variability and consider its implications when designing TB antibiotics and vaccines in the future.

1. Herzog, H. (1998) History of tuberculosis, *Respiration 65*, 5-15.
2. (2009) WHO health statistics 2009. The World Health Organization.
3. Manosuthi, W. et al. (2006) Survival rate and risk factors of mortality among HIV/tuberculosis-coinfected patients with and without antiretroviral therapy, *Journal of Acquired Immune Deficiency Syndromes 43*, 42-46.
4. Raviglione, M.C. et al. (1995) Global epidemiology of tuberculosis. Morbidity and mortality of a worldwide epidemic, *Journal of the American Medical Association 273*, 220-226.
5. Jones, D. et al. (1944) Control of gram-negative bacteria in experimental animals by streptomycin, *Science 100*, 103-105.
6. Cole, S.T. et al. (1998) Deciphering the biology of Mycobacterium tuberculosis from the complete genome sequence. *Nature 393*, 537-544.
7. Long, R. (2007) *Canadian Tuberculosis Standards*, 6th ed., Public Health Agency of Canada.
8. Diedrich, C.R., and Flynn, J.A.L. (2011) HIV-1/Mycobacterium tuberculosis Coinfection Immunology: How Does HIV-1 Exacerbate Tuberculosis?, *Infection and Immunity 79*, 1407-1417.
9. Kogieleum, N. et al. (2010) HIV-Associated Tuberculosis, *Clinical and Developmental Immunology 2011*. 1-8.
10. Chiang, C.Y. et al. (2010) Drug-resistant tuberculosis: past, present, future, *Respirology 15*, 413-432.
11. Cardona, P. J. (2009) A Dynamic Reinfection Hypothesis of Latent Tuberculosis Infection, *Infection 37*, 80-86.
12. Zhang, Y. (2005) The magic bullets and tuberculosis drug targets, *Annual Review of Pharmacology and Toxicology 45*, 529-564.
13. Brosch, R. et al. (2007) Genome plasticity of BCG and impact on vaccine efficacy, *Proceedings of the National Academy of Sciences 104*, 5596-5601.
14. Becq, J. et al. (2007) Contribution of horizontally acquired genomic islands to the evolution of the tubercle bacilli, *Molecular Biology and Evolution 24*, 1861-1871.
15. Alland, D. et al. (2003) Modeling bacterial evolution with comparative-genome-based marker systems: application to Mycobacterium tuberculosis evolution and pathogenesis, *Journal of Bacteriology 185*, 3392-3399.
16. Hart, P.D., and Sutherland, I. (1977) BCG and vole bacillus vaccines in the prevention of tuberculosis in adolescence and early adult life, *British Medical Journal 2*, 293-295.
17. Comstock, G.W., and Palmer, C.E. (1966) Long-term results of BCG vaccination in the southern United States, *American Review of Respiratory Disease 93*, 171-183.
18. (1979) Trial of BCG vaccines in south India for tuberculosis prevention, *Indian Journal of Medical Research 70*, 349-363.

19. Nicas, M. et al. (2005) Toward understanding the risk of secondary airborne infection: emission of respirable pathogens, *Journal of Occupational and Environmental Hygiene 2*, 143-154.
20. Dean, G.S. et al. (2005) Minimum infective dose of Mycobacterium bovis in cattle, *Infection and Immunity 73*, 6467-6471.
21. Schwartzman, K. (2002) Latent tuberculosis infection: old problem, new priorities, *Canadian Medical Association Journal 166*, 759-761.
22. Pieters, J. (2008) Mycobacterium tuberculosis and the macrophage: maintaining a balance, *Cell Host and Microbe 3*, 399-407.
23. Russell, D.G. (2001) Mycobacterium tuberculosis: here today, and here tomorrow, *Nature Reviews Molecular Cell Biology 2*, 569-577.
24. van der Wel, N. et al. (2007) M. tuberculosis and M. leprae translocate from the phagolysosome to the cytosol in myeloid cells, *Cell 129*, 1287-1298.
25. Hagedorn, M. et al. (2009) Infection by tubercular mycobacteria is spread by nonlytic ejection from their amoeba hosts, *Science 323*, 1729-1733.
26. Anderson, J.M. (2000) Multinucleated giant cells, *Current Opinion in Hematology 7*, 40-47.
27. Wayne, L.G., and Sohaskey, C.D. (2001) Nonreplicating persistence of mycobacterium tuberculosis, *Annual Review of Microbiology 55*, 139-163.
28. Bold, T.D., and Ernst, J.D. (2009) Who Benefits from Granulomas, Mycobacteria or Host?, *Cell 136*, 17-19.
29. Davis, J.M., and Ramakrishnan, L. (2009) The Role of the Granuloma in Expansion and Dissemination of Early Tuberculous Infection, *Cell 136*, 37-49.
30. Comas, I. et al. (2010) Human T cell epitopes of Mycobacterium tuberculosis are evolutionarily hyperconserved, *Nature Genetics 42*, 498-503.
31. Chao, M.C., and Rubin, E.J. (2010) Letting sleeping dos lie: does dormancy play a role in tuberculosis?, *Annual Review of Microbiology 64*, 293-311.
32. Lillebaek, T. et al. (2002) Molecular evidence of endogenous reactivation of Mycobacterium tuberculosis after 33 years of latent infection, *Journal of Infectious Diseases 185*, 401-404.
33. Zhang, Y. (2004) Persistent and dormant tubercle bacilli and latent tuberculosis, *Frontiers in Bioscience 9*, 1136-1156.
34. Corper, H.J., and Cohn, M.L. (1951) The viability and virulence of old cultures of tubercle bacilli; studies on 30-year-old broth cultures maintained at 37 degrees C, *Tubercle 32*, 232-237.
35. Rustad, T.R. et al. (2009) Hypoxia: a window into Mycobacterium tuberculosis latency, *Cellular Microbiology 8*, 1151-1159.
36. Olender, S. et al. (2003) Low prevalence and increased household clustering of Mycobacterium tuberculosis infection in high altitude villages in Peru, *The American Journal of Tropical Medicine and Hygiene 68*, 721-727.
37. Wayne, L.G., and Hayes, L.G. (1996) An in vitro model for sequential study of shiftdown of Mycobacterium tuberculosis through two stages of nonreplicating persistence, *Infection and Immunity 64*, 2062-2069.
38. Rustad, T.R. et al. (2008) The enduring hypoxic response of Mycobacterium tuberculosis, *PLoS ONE 3*, e1502.

39. Brosch, R. et al. (2002) A new evolutionary scenario for the Mycobacterium tuberculosis complex, *Proceedings of the National Academy of Sciences 99*, 3684-3689.
40. Kremer, L., and Besra, G.S. (2005) *A waxy tale, by Mycobacterium tuberculosis*, ASM Press: Washington DC.
41. Liu, J. et al. (1996) Mycolic acid structure determines the fluidity of the mycobacterial cell wall, *Journal of Biological Chemistry 271*, 29545-29551.
42. Barry, C.E. et al. (1998) Mycolic acids: structure, biosynthesis and physiological functions, *Progress in Lipid Research 37*, 143-179.
43. Lima, V.M.F. et al. (2001) Role of trehalose dimycolate in recruitment of cells and modulation of production of cytokines and NO in tuberculosis, *Infection and Immunity 69*, 5305-5312.
44. Chatterjee, D., and Khoo, K.H. (1998) Mycobacterial lipoarabinomannan: an extraordinary lipoheteroglycan with profound physiological effects, *Glycobiology 8*, 113-120.
45. Zhang, L. et al. (1988) Effect of Mycobacterium tuberculosis-derived sulfolipid I on human phagocytic cells, *Infection and Immunity 56*, 2876-2883.
46. Rousseau, C. et al. (2004) Production of phthiocerol dimycocerosates protects Mycobacterium tuberculosis from the cidal activity of reactive nitrogen intermediates produced by macrophages and modulates the early immune response to infection, *Cellular Microbiology 6*, 277-287.
47. Reed, M.B., et al. (2004) A glycolipid of hypervirulent tuberculosis strains that inhibits the innate immune response, *Nature 431*, 84-87.
48. Rhee, K.Y. et al. (2011) Central carbon metabolism in Mycobacterium tuberculosis: an unexpected frontier, *Trends Microbiol*ogy 19, 307-314.
49. Pandey, A.K., and Sassetti, C.M. (2008) Mycobacterial persistence requires the utilization of host cholesterol, *Proceedings of the National Academy of Sciences 105*, 4376-4380.
50. Sassetti, C.M., and Rubin, E.J. (2003) Genetic requirements for mycobacterial survival during infection, *Proceedings of the National Academy of Sciences 100*, 12989-12994.
51. Schnappinger, D. et al. (2003) Transcriptional Adaptation of Mycobacterium tuberculosis within Macrophages: Insights into the Phagosomal Environment, *Journal of Experimental Medicine 198*, 693-704.
52. Timm, J. et al. (2003) Differential expression of iron-, carbon-, and oxygen-responsive mycobacterial genes in the lungs of chronically infected mice and tuberculosis patients, *Proceedings of the National Academy of Sciences 100*, 14321-14326.
53. de Carvalho, L.P. et al. (2010) Metabolomics of Mycobacterium tuberculosis reveals compartmentalized co-catabolism of carbon substrates, *Chemistry and Biology 17*, 1122-1131.
54. Voskuil, M.I. et al. (2003) Inhibition of respiration by nitric oxide induces a Mycobacterium tuberculosis dormancy program, *Journal of Experimental Medicine 198*, 705-713.

55. Hu, Y. et al. (2006) Deletion of the Mycobacterium tuberculosis {alpha}-crystallin-like hspX gene causes increased bacterial growth in vivo, *Infection and Immunity 74*, 861-868.
56. Voskuil, M. I. et al. (2004) Mycobacterium tuberculosis gene expression during adaptation to stationary phase and low-oxygen dormancy, *Tuberculosis 84*, 218-227.
57. Sharma, D. et al. (2006) Expression of mycobacterial cell division protein, FtsZ, and dormancy proteins, DevR and Acr, within lung granulomas throughout guinea pig infection, *Immunology and Medical Microbiology 48*, 329-336.
58. Karakousis, P.C. et al. (2004) Dormancy phenotype displayed by extracellular Mycobacterium tuberculosis within artificial granulomas in mice, *Journal of Experimental Medicine 200*, 647-657.
59. Kumar, A. et al. (2008) Heme oxygenase-1-derived carbon monoxide induces the Mycobacterium tuberculosis dormancy regulon, *Journal of Biological Chemistry 283*, 18032-18039.
60. Pang, X. et al. (2007) Evidence for complex interactions of stress-associated regulons in an mprAB deletion mutant of Mycobacterium tuberculosis, *Microbiology 153*, 1229-1242.
61. Rohde, K. et al. (2007) Mycobacterium tuberculosis and the environment within the phagosome, *Immunological Reviews 219*, 37-54.
62. Leistikow, R.L. et al. (2009) The Mycobacterium tuberculosis DosR regulon assists in metabolic homeostasis and enables rapid recovery from non-respiring dormancy, *J Bacteriol 192*, 1662-1670.
63. Gagneux, S., and Small, P.M. (2007) Global phylogeography of Mycobacterium tuberculosis and implications for tuberculosis product development, *Lancet Infectious Disseases 7*, 328-337.
64. Sreevatsan, S. et al. (1997) Restricted structural gene polymorphism in the Mycobacterium tuberculosis complex indicates evolutionarily recent global dissemination, *Proceedings of the National Academy of Sciences 94*, 9869-9874.
65. Hershberg, R. et al. (2008) High functional diversity in Mycobacterium tuberculosis driven by genetic drift and human demography, *PLoS Biology 6*, e311.
66. Schurch, A.C. et al. (2011) Mutations in the regulatory network underlie the recent clonal expansion of a dominant subclone of the Mycobacterium tuberculosis Beijing genotype, *Infection, Genetics and Evolution 11*, 587-597.
67. Stinear, T.P. et al. (2008) Insights from the complete genome sequence of Mycobacterium marinum on the evolution of Mycobacterium tuberculosis, *Genome Research 18*, 729-741.
68. Filliol, I. et al. (2006) Global phylogeny of Mycobacterium tuberculosis based on single nucleotide polymorphism (SNP) analysis: insights into tuberculosis evolution, phylogenetic accuracy of other DNA fingerprinting systems, and recommendations for a minimal standard SNP set, *Journal of Bacteriology 188*, 759-772.

69. Gagneux, S. et al. (2006) Variable host-pathogen compatibility in Mycobacterium tuberculosis, *Proceedings of the National Academy of Sciences 103*, 2869-2873.
70. Reed, M.B. et al. (2009) Major Mycobacterium tuberculosis lineages associate with patient country of origin, *Journal of Clinical Microbiology 47*, 1119-1128.
71. Parwati, I. et al. (2010) Possible underlying mechanisms for successful emergence of the Mycobacterium tuberculosis Beijing genotype strains, *Lancet Infectious Disseases 10*, 103-111.
72. van der Spuy, G.D. et al. (2009) Changing Mycobacterium tuberculosis population highlights clade-specific pathogenic characteristics, *Tuberculosis 89*, 120-125.
73. Reed, M.B. et al. (2007) The W-Beijing lineage of Mycobacterium tuberculosis overproduces triglycerides and has the DosR dormancy regulon constitutively upregulated, *Journal of Bacteriology 189*, 2583-2589.
74. Kremer, K. et al. (2009) Vaccine-induced immunity circumvented by typical Mycobacterium tuberculosis Beijing strains, *Emerging Infectious Diseases 15*, 335-339.
75. Lopez, B. et al. (2003) A marked difference in pathogenesis and immune response induced by different Mycobacterium tuberculosis genotypes, *Clinical and Experimental Immunology 133*, 30-37.
76. Tsenova, L. et al. (2007) BCG vaccination confers poor protection against M. tuberculosis HN878-induced central nervous system disease, *Vaccine 25*, 5126-5132.
77. Devaux, I. et al. (2009) Clusters of multidrug-resistant Mycobacterium tuberculosis cases, Europe, *Emerging Infectious Diseases 15*, 1052-1060.
78. Hillemann, D. et al. (2005) Disequilibrium in distribution of resistance mutations among Mycobacterium tuberculosis Beijing and non-Beijing strains isolated from patients in Germany, *Antimicrobial Agents and Chemotherapy 49*, 1229-1231.
79. Mokrousov, I. et al. (2002) Detection of embB306 mutations in ethambutol-susceptible clinical isolates of Mycobacterium tuberculosis from Northwestern Russia: implications for genotypic resistance testing, *Journal of Clinical Microbiology 40*, 3810-3813.
80. Manca, C. et al. (2004) Differential monocyte activation underlies strain-specific Mycobacterium tuberculosis pathogenesis, *Infection and Immunity 72*, 5511-5514.
81. Caws, M. et al. (2008) The influence of host and bacterial genotype on the development of disseminated disease with Mycobacterium tuberculosis, *PloS Pathogens 4*, e1000034.
82. van Crevel, R. et al. (2009) Infection with Mycobacterium tuberculosis Beijing genotype strains is associated with polymorphisms in SLC11A1/NRAMP1 in Indonesian patients with tuberculosis, *Journal of Infectious Diseases 200*, 1671-1674.
83. Behar, S.M. et al. (2011) Apoptosis is an innate defense function of macrophages against Mycobacterium tuberculosis, *Mucosal Immunology 4*, 279-287.

84. Sohn, H. et al. (2009) Induction of cell death in human macrophages by a highly virulent Korean Isolate of Mycobacterium tuberculosis and the virulent strain H37Rv, *Scandinavian Journal of Immunology 69*, 43-50.
85. Dormans, J. et al. (2004) Correlation of virulence, lung pathology, bacterial load and delayed type hypersensitivity responses after infection with different Mycobacterium tuberculosis genotypes in a BALB/c mouse model, *Clinical & Experimental Immunology 137*, 460-468.
86. Tsenova, L. et al. (2005) Virulence of selected Mycobacterium tuberculosis clinical isolates in the rabbit model of meningitis is dependent on phenolic glycolipid produced by the bacilli, *Journal of Infectious Diseases 192*, 98-106.
87. Kong, Y. et al. (2007) Association between Mycobacterium tuberculosis Beijing/W lineage strain infection and extrathoracic tuberculosis: insights from epidemiologic and clinical characterization of the three principal genetic groups of M. tuberculosis clinical isolates, *Journal of Clinical Microbiology 45*, 409-414.
88. de Jong, B.C. et al. (2008) Progression to active tuberculosis, but not transmission, varies by Mycobacterium tuberculosis lineage in The Gambia, *Journal of Infectious Diseases 198*, 1037-1043.
89. Them, S. et al. (2007) Beijing family Mycobacterium tuberculosis strains differ in their intracellular growth in THP-1 macrophages, *International Journal of Tuberculosis and Lung Disease 11*, 1087-1093.
90. Pheiffer, C. et al. (2005) Protein expression by a Beijing strain differs from that of another clinical isolate and Mycobacterium tuberculosis H37Rv, *Microbiology 151*, 1139-1150.
91. Mitrophanov, A.Y. et al. (2008) Signal integration in bacterial two-component regulatory systems, *Genes and Development 22*, 2601-2611.
92. Gao, R. et al. (2007) Bacterial response regulators: versatile regulatory strategies from common domains, *Trends in Biochemical Sciences 32*, 225-234.
93. Wisedchaisri, G. et al. (2008) Crystal structures of the response regulator DosR from Mycobacterium tuberculosis suggest a helix rearrangement mechanism for phosphorylation activation, *Journal of Molecular Biology 378*, 227-242.
94. Stock, A.M. et al. (2000) Two-component signal transduction, *Annual Review of Biochemistry 69*, 183-215.
95. Burkholder, W.F. et al. (2001) Replication initiation proteins regulate a developmental checkpoint in Bacillus subtilis, *Cell 104*, 269-279.
96. Perego, M., and Brannigan, J.A. (2001) Pentapeptide regulation of aspartyl-phosphate phosphatases, *Peptides 22*, 1541-1547.
97. Ogino, T. et al. (1998) An Escherichia coli protein that exhibits phosphohistidine phosphatase activity towards the HPt domain of the ArcB sensor involved in the multistep His-Asp phosphorelay, *Molecular Microbiology 27*, 573-585.
98. Kato, A., and Groisman, E.A. (2004) Connecting two-component regulatory systems by a protein that protects a response regulator from

dephosphorylation by its cognate sensor, *Genes and Development 18*, 2302-2313.
99. Eguchi, Y. et al. (2007) B1500, a small membrane protein, connects the two-component systems EvgS/EvgA and PhoQ/PhoP in Escherichia coli, *Proceedings of the National Academy of Sciences 104*, 18712-18717.
100. Core, L., and Perego, M. (2003) TPR mediated interaction of RapC with ComA inhibits response regulator DNA binding for competence development in Bacillus subtilis, *Mol Microbiol 49*, 1509-1522.
101. Nakano, S. et al. (2003) A regulatory protein that interferes with activator-stimulated transcription in bacteria, *Proceedings of the National Academy of Sciences 100*, 4233-4238.
102. Tu, X. et al. (2006) The PhoP/PhoQ two-component system stabilizes the alternative sigma factor RpoS in Salmonella enterica, *Proceedings of the National Academy of Sciences 103*, 13503-13508.
103. Av-Gay, Y., and Everett, M. (2000) The eukaryotic-like Ser/Thr protein kinases of Mycobacterium tuberculosis, *Trends in Microbiology 8*, 238-244.
104. Tucker, P.A. et al. (2007) Two-component systems of Mycobacterium tuberculosis: structure-based approaches, *Methods in Enzymology 423*, 479-501.
105. Chao, J.D. et al. (2010) Convergence of Ser/Thr and two-component signaling to coordinate expression of the dormancy regulon in Mycobacterium tuberculosis, *J Biol Chem 285*, 29239-29246.
106. Dasgupta, N. et al. (2000) Characterization of a two-component system, devR-devS, of Mycobacterium tuberculosis, *Tubercule 80*, 141-159.
107. Roberts, D.M. et al. (2004) Two sensor kinases contribute to the hypoxic response of Mycobacterium tuberculosis, *Journal of Biological Chemistry 279*, 23082-23087.
108. Boon, C., and Dick, T. (2002) Mycobacterium bovis BCG response regulator essential for hypoxic dormancy, *Journal of Bacteriology 184*, 6760-6767.
109. Sherman, D.R. et al. (2001) Regulation of the Mycobacterium tuberculosis hypoxic response gene encoding alpha -crystallin, *Proceedings of the National Academy of Sciences 98*, 7534-7539.
110. Sousa, E.H. et al. (2007) DosT and DevS are oxygen-switched kinases in Mycobacterium tuberculosis, *Protein Science 16*, 1708-1719.
111. Aravind, L., and Ponting, C.P. (1997) The GAF domain: an evolutionary link between diverse phototransducing proteins, *Trends in Biochemical Sciences 22*, 458-459.
112. Sardiwal, S. et al. (2005) A GAF domain in the hypoxia/NO-inducible Mycobacterium tuberculosis DosS protein binds haem, *Journal of Molecular Biology 353*, 929-936.
113. Saini, D.K. et al. (2004) Cross talk between DevS sensor kinase homologue, Rv2027c, and DevR response regulator of Mycobacterium tuberculosis, *FEBS Letters 565*, 75-80.
114. Ioanoviciu, A. et al. (2007) DevS, a heme-containing two-component oxygen sensor of Mycobacterium tuberculosis, *Biochemistry 46*, 4250-4260.

115. Yukl, E.T. et al. (2007) Interdomain interactions within the two-component heme-based sensor DevS from Mycobacterium tuberculosis, *Biochemistry 46*, 9728-9736.
116. Kumar, A. et al. (2007) Mycobacterium tuberculosis DosS is a redox sensor and DosT is a hypoxia sensor, *Proceedings of the National Academy of Sciences 104*, 11568-11573.
117. Yukl, E.T. et al. (2011) Nitric oxide dioxygenation reaction in DevS and the initial response to nitric oxide in Mycobacterium tuberculosis, *Biochemistry 50*, 1023-1028.
118. Honaker, R.W. et al. (2010) DosS responds to a reduced electron transport system to induce the Mycobacterium tuberculosis DosR regulon, *Journal of Bacteriology 192,* 6447-6455.
119. Cho, H.Y. et al. (2009) Structural insight into the heme-based redox sensing by DosS from Mycobacterium tuberculosis, *Journal of Biological Chemistry 284*, 13057-13067.
120. Saini, D.K. et al. (2002) Cloning, overexpression, purification, and matrix-assisted refolding of DevS (Rv 3132c) histidine protein kinase of Mycobacterium tuberculosis, *Protein Expression and Purification 25*, 203-208.
121. Wisedchaisri, G. et al. (2005) Structures of Mycobacterium tuberculosis DosR and DosR-DNA complex involved in gene activation during adaptation to hypoxic latency, *Journal of Molecular Biology 354*, 630-641.
122. Park, H.D. et al. (2003) Rv3133c/dosR is a transcription factor that mediates the hypoxic response of Mycobacterium tuberculosis, *Molecular Microbiology 48*, 833-843.
123. Chauhan, S., and Tyagi, J. S. (2008) Interaction of DevR with multiple binding sites synergistically activates divergent transcription of narK2-Rv1738 genes in Mycobacterium tuberculosis, *Journal of Bacteriology 190*, 5394-5403.
124. Chauhan, S., and Tyagi, J. S. (2008) Cooperative binding of phosphorylated DevR to upstream sites is necessary and sufficient for activation of the Rv3134c-devRS operon in Mycobacterium tuberculosis: implication in the induction of DevR target genes, *Journal of Bacteriology 190*, 4301-4312.
125. Rodriguez, J. G. et al. (2008) Rv3134c/devR/devS operon of Mycobacterium bovis BCG is differentially transcribed under "in vitro" stress conditions, *Tuberculosis 88*, 273-282.
126. Parish, T. et al. (2003) Deletion of two-component regulatory systems increases the virulence of Mycobacterium tuberculosis, *Infection and Immunity 71*, 1134-1140.
127. Malhotra, V. et al. (2004) Disruption of response regulator gene, devR, leads to attenuation in virulence of Mycobacterium tuberculosis, *FEMS Microbiology Letters 231*, 237-245.
128. Converse, P. J. et al. (2009) Role of the dosR-dosS two-component regulatory system in Mycobacterium tuberculosis virulence in three animal models, *Infection and Immunity 77*, 1230-1237.
129. Homolka, S. et al. (2010) Functional genetic diversity among Mycobacterium tuberculosis complex clinical isolates: delineation of conserved core and

lineage-specific transcriptomes during intracellular survival, *PLoS Pathogens 6*, e1000988.
130. Badillo-Lopez, C. et al. (2010) Differential expression of dnaA and dosR genes among members of the Mycobacterium tuberculosis complex under oxic and hypoxic conditions, *International Microbiology 13*, 9-13.
131. Fallow, A. et al. (2010) Strains of the East Asian (W/Beijing) lineage of Mycobacterium tuberculosis are DosS/DosT-DosR two-component regulatory system natural mutants, *Journal of Bacteriology 192*, 2228-2238.
132. Murry, J.P et al. (2005) A new site-specific integration system for mycobacteria, *Tuberculosis 85*, 317-323.
133. Murry, J. P. et al. (2008) Transposon site hybridization in Mycobacterium tuberculosis, *Methods in Molecular Biology 416*, 45-59.
134. Mayuri et al. (2002) Molecular analysis of the dormancy response in Mycobacterium smegmatis: expression analysis of genes encoding the DevR-DevS two-component system, Rv3134c and chaperone alpha-crystallin homologues, *FEMS Microbiology Letters 211*, 231-237.
135. Galagan, J.E. et al. (2010) TB database 2010: overview and update, *Tuberculosis 90*, 225-235.
136. Lew, J.M. et al. (2011) TubercuList-10 years after, *Tuberculosis 91*, 1-7.
137. Pym, A.S. et al. (2001) Regulation of catalase peroxidase (KatG) expression, isoniazid sensitivity and virulence by furA of Mycobacterium tuberculosis, *Molecular Microbiology 40*, 879-889.
138. Hassett, D. et al. (2000) Hydrogen peroxide sensitivity of catechol-2, 3-dioxygenase: a cautionary note on use of xylE reporter fusions under aerobic conditions, *Applied and Environmental Microbiology 66*, 4119-4123.
139. Shatalin, K. et al. (2008) Bacillus anthracis-derived nitric oxide is essential for pathogen virulence and survival in macrophages, *Proceedings of the National Academy of Sciences 105*, 1009-1013.
140. Mukamolova, G.V. et al. (2002) A family of autocrine growth factors in Mycobacterium tuberculosis, *Molecular Microbiology 46*, 623-635.
141. Manca, C. et al. (1999) Mycobacterium tuberculosis catalase and peroxidase activities and resistance to oxidative killing in human monocytes in vitro, *Infection and Immunity 67*, 74-79.
142. Seaver, L.C., and Imlay, J.A. (2001) Alkyl hydroperoxide reductase is the primary scavenger of endogenous hydrogen peroxide in Escherichia coli, *Journal of Bacteriology 183*, 7173-7181.